

19. SITE 943¹

Shipboard Scientific Party²

HOLE 943A

Date occupied: 11 May 1994
Date departed: 12 May 1994
Time on hole: 1 day, 1 hr, 45 min
Position: 5°56.808'N, 47°46.831'W
Bottom felt (drill pipe measurement from rig floor, m): 3749.7
Distance between rig floor and sea level (m): 11.30
Water depth (drill pipe measurement from sea level, m): 3738.5
Penetration (m): 106.30
Number of cores (including cores having no recovery): 12
Total length of cored section (m): 106.30
Total core recovered (m): 66.46
Core recovery (%): 62
Oldest sediment cored:
Depth (mbsf): 106.30
Nature: Silty clay
Earliest age: Pleistocene

Principal results: Site 943 (proposed Site AF-23) is located in the main (Amazon) channel on the central part of the Amazon Fan. It was intended to sample the coarsest sediment transported by recent turbidity current flows within the constraints of a known channel geometry and to determine the nature of the high-amplitude reflections (HARs) that underlie the channel in seismic profiles. Nearby Site 944 (proposed Site AF-3) sampled the levee of this channel.

The site was selected from a *Conrad* seismic-reflection profile (C2514; 0605UTC on 4 Dec.) and multibeam bathymetry. The precise position was determined by pre-site survey from the *JOIDES Resolution*. The site is in a straight reach of the channel 2 km down-channel from the *Conrad* seismic profile and on our *JOIDES Resolution* profile.

Hole 943A was cored by APC to 40.2 mbsf, then by XCB to 106.3 mbsf. Total hole recovery was 66.46 m (62.5%). No temperature measurements were made. There was gas expansion in many cores. Methane was found throughout the hole, but higher hydrocarbons were not detected.

Four lithologic units are recognized:

Unit I (0–1.58 mbsf) is a Holocene, bioturbated, brown nannofossil-foraminifer clay, similar to that observed at other Leg 155 sites, that is interbedded with a 73-cm-thick interval containing a mass-flow deposit and silt-clay turbidite(s), which may be slumped. An iron-rich diagenetic crust is developed at 1.28 mbsf. A gray foraminifer-nannofossil clay occurs at the base of the unit.

Unit II (1.58–6.26 mbsf) comprises bioturbated mud with increasing amounts of black hydrotroilite staining below 3 mbsf, associated with a high total sulfur content (0.77%).

Unit III (6.26–62.88) consists of mud with interbedded sand. Recovery was only 48%, and some recovered sand appeared to be flow-in. At the top of the unit, a fine sand with millimeter-size plant fragments was recovered in two cores, but its original thickness is unknown, and it may be mostly flow-in. A large clast of nannofossil-bearing clay occurs at the top of the sand. An interval from 32.8–40.2 mbsf recovered mud with abundant beds of silt and sand, commonly with erosive bases. There is a general trend toward thicker beds in the lower part of the interval. The thickest bed recovered is an 81-cm-thick silt bed with mud clasts. In the lower part of the unit, a thick bed of silt with minor mud clasts overlies a 19-cm-thick graded bed from very coarse sand to silt, which is underlain by a 2-m-thick bed containing clasts of mud with silt laminae set in a coarse sand matrix.

Unit IV (67.80–106.25) consists of mud with laminae and thin beds of silt. It is divided into subunits on the basis of the frequency of silt laminae and beds. Subunit IVA (to 89.19 mbsf) has abundant silt beds and laminae. Subunit IVB (to 93.29) comprises mottled mud, locally with color banding. Subunit IVC (to base of unit) consists of color-banded mud with frequent beds and laminae of silt. Siderite bands are present in this subunit. Subunit IVA corresponds to levee deposits of the Brown Channel-levee System, whereas Subunits IVB and IVC appear to correlate with the Purple Channel-levee System.

Foraminifer and nannofossil abundances are generally high in Unit I, except in the resedimented deposits, and low throughout the remaining units. *P. obliquiloculata* was not found below the Holocene section, suggesting an age <40 ka for the base of the hole.

This site has provided a channel-fill section through the Amazon Channel on the lower mid-fan that can be compared with Site 934, 60 km up-fan. The channel-fill sequence is about 60 m thick, with coarse sand near its base. Otherwise no sediment coarser than fine sand was recovered. The channel overlies levee sediment, suggesting that it has shifted laterally as the levee has accreted. Correlation with levee sediment of adjacent Site 944 will provide information on the nature of turbidity currents that flowed through the channel and overspilled its levees.

SETTING AND OBJECTIVES

Introduction

Site 943 (proposed Site AF-23) is located in the main (Amazon) channel of the Amazon Fan, on the lower part of the middle fan at a water depth of 3735 m. By sampling in the channel we can potentially sample the coarsest sediment transported by latest Pleistocene turbidity currents at this depth on the fan, within the constraints of a known channel geometry. Also, we can determine the nature of the high-amplitude reflections (HARs) that underlie the channel in seismic profiles. Nearby Site 944 sampled the levee of this channel as well as deeper layers that extend beneath the channel and levee.

Setting

Site 943 is located in the most recently active Amazon Fan channel (Figs. 1 and 2). Channel geometry and near-surface sedimentation

¹Flood, R.D., Piper, D.J.W., Klaus, A., et al., 1995. *Proc. ODP, Init. Repts.*, 155: College Station, TX (Ocean Drilling Program).

²Shipboard Scientific Party is as given in the list of participants in the contents.

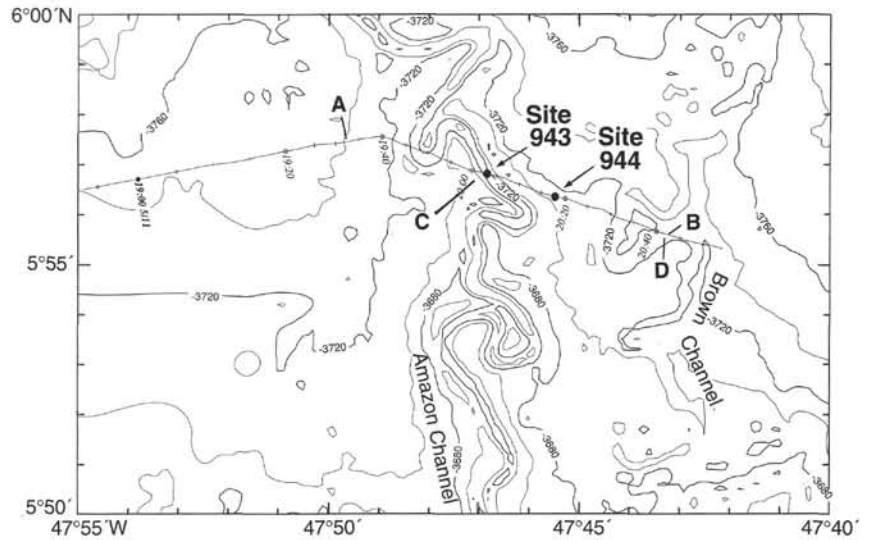


Figure 1. SeaBeam bathymetric map (in meters) of the channel and levee of the Amazon Channel. Locations of Sites 943 and 944 and profiles A–B and C–D are shown.

patterns have been studied in this area with multibeam bathymetry and piston cores (Flood et al., 1991; Pirmez, 1994). The position of Site 943 in the channel was verified by 3.5-kHz profiler and by the length of drill pipe to the mud line; however, the position of the hole relative to the channel walls is unknown. The channel in the vicinity of Site 943 is about 200 m wide, 75 m deep, and nearly straight for 2 km in both up-channel and down-channel directions. Channel sinuosity in this region is 2.5 and the along-channel gradient of the present-day channel floor is 2 m/km (Flood and Damuth, 1987; Pirmez, 1994).

Site 943 was positioned near a *Conrad* seismic line (C2514, 0605UTC on 4 Dec. 1984). Our *JOIDES Resolution* seismic profile crossed the site at 2003UTC on 11 May 1994 (Fig. 3). The 3.5-kHz profile shows 12 ms of sub-bottom reflectors in the channel that may be finer grained fill (Fig. 2). Seismic profiles in the vicinity of the channel are difficult to interpret because side-echoes from the meandering channel are superimposed on reflections from beneath the channel (Flood, 1987). In particular, the HARs commonly observed beneath the channel on seismic profiles (e.g., Fig. 3) are thought to be caused in part by side echoes (Flood, 1987).

Objectives

The principal objectives of coring at Site 943 were:

1. Sampling and characterization of channel-floor sediment in the most recently active channel.
2. Characterizing the sequence of sediment that fills the channel.
3. Sampling sediment related to the earliest stages of channel formation and evolution.
4. Characterization of turbidity current flow through analysis of turbidite characteristics and comparison to the adjacent Site 944 on the levee crest.

OPERATIONS

Transit: Site 942 to Site 943 (AF-23)

The 76-nmi transit from Site 942 to 943 took 7.6 hr. We conducted a short seismic-reflection survey to confirm the original survey position. At 1756 hr 11 May, we deployed a beacon at 5°56.816'N, 47°46.827'W.

Hole 943A

We decided to use the XCB flow control valve because the test results at Hole 942A indicated that the device would not reduce recovery. We suspected that the sticky clay might plug the bit nozzles. A

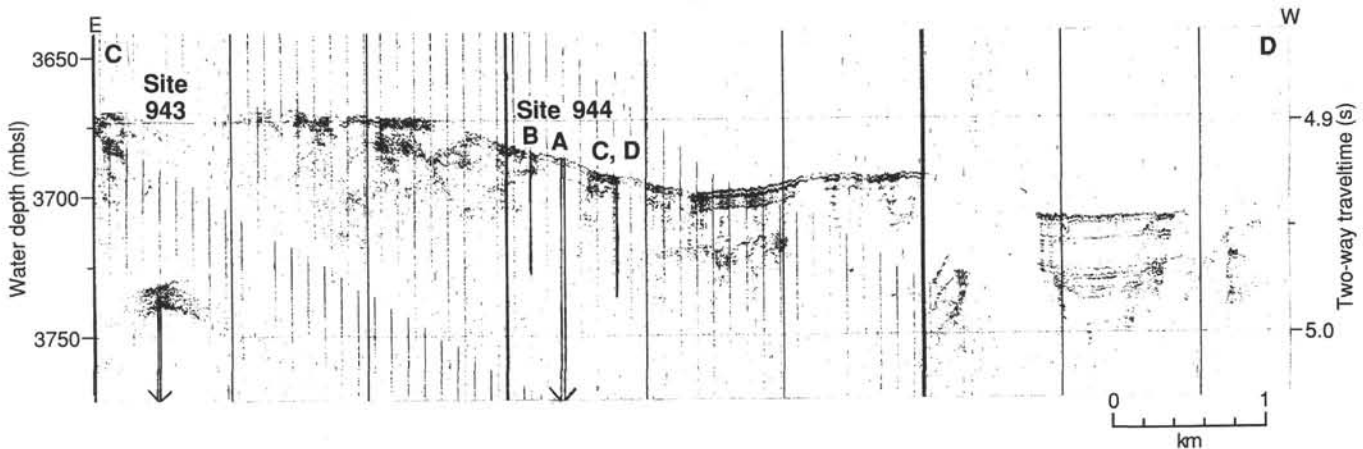


Figure 2. A 3.5-kHz profile C–D across Sites 943 and 944 (*JOIDES Resolution* 2000–2044 UTC 11 May 1994).

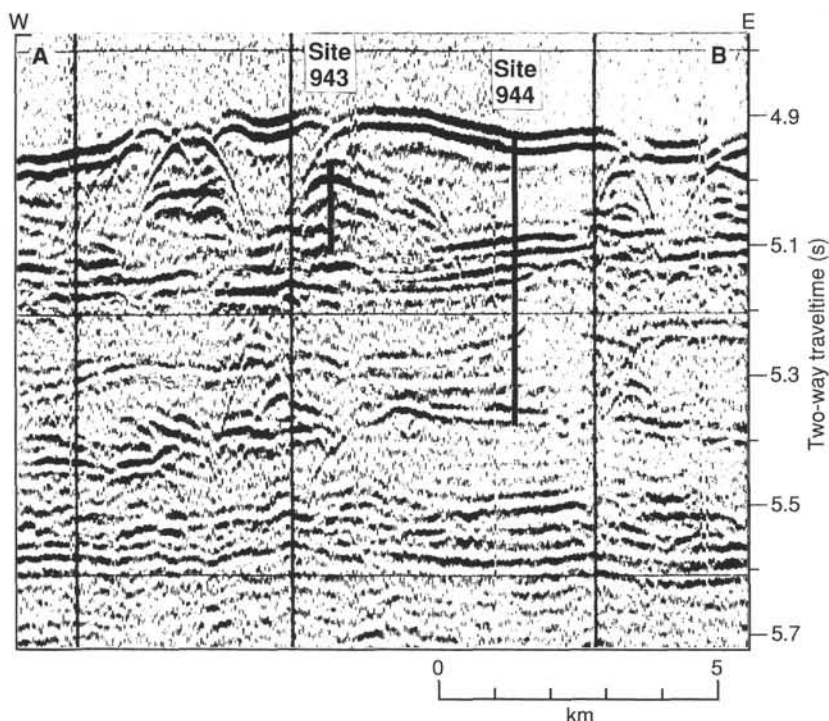


Figure 3. Seismic profile A-B across the Amazon Channel-levee System, including Sites 943 and 944 (JOIDES Resolution 1933–2044 UTC 11 May 1994).

lockable flapper valve was run because we planned to move in dynamic positioning mode to Site 944, where logging was planned.

We positioned the bit at 3744.5 mbrf and spudded Hole 943A at 0108 hr 12 May. Core 1H recovered 4.27 m, and the mud line was defined to be at 3749.7 mbrf. The distance from sea level to rig floor, which depends on the ship's draft, was 11.26 m for Hole 943A. Cores 1H through 5H were taken from 3749.7 to 3789.9 mbrf (0–40.2 mbsf) and recovered 29.94 m (75%; Table 1). Cores 3H through 5H were oriented with the Tensor tool. Part of Core 2H was lost due to a crushed core liner. Cores 3H through 5H were partial strokes with 20,000- to 30,000-lb overpull, and the APC apparently was unable to penetrate the sand.

XCB Cores 6X through 12X were taken from 3789.9 to 3856.0 mbrf (40.2–106.3 mbsf), coring 66.1 m and recovering 36.52 m (55%). The overall APC/XCB recovery was 63%. The flow control valve was run in defeated mode on alternate cores. It was not clear whether the flow control valve had any effect on core recovery. Cor-

ing parameters were 10,000-lb weight-on-bit at 80 rpm with 125–300 amp torque, while pumping little seawater (“dry coring” with 0–35 gpm) at 0–150 psi. The formation was predominantly unconsolidated sand. The bit cleared the seafloor, and we recovered the beacon at 1945 hr 12 May.

LITHOSTRATIGRAPHY

Introduction

Hole 943A, which is located in the main Amazon Channel on the central part of the fan, recovered sediment from a maximum depth of 106.25 mbsf. Recovery was variable downhole ranging from 0% to 100% with an average of 62% (Figs. 4 and 5). Expansion of methane gas during core recovery commonly affected the sediment by disrupting the primary sedimentary structures in many silt and sand beds, and by producing void spaces within some of the core sections (see “Lithostratigraphy” section in the “Explanatory Notes” chapter, this volume). In addition, most of the sand recovered with the APC was soupy and therefore structureless as a result of “flow-in”.

Description of Lithostratigraphic Units

Unit I

Interval: 155-943A-1H-1, 0 cm, through -1H-2, 8 cm
Age: Holocene
Depth: 0.00–1.58 mbsf

Unit I consists of calcareous clay intervals similar to those observed at most other sites on the surface of the Amazon Fan but with interbedded terrigenous sediment. The top 6 cm are brown (10YR 4/3) nannofossil-foraminifer-rich clay, which has a carbonate content of 10.4% (see “Organic Geochemistry” section, this chapter), and which overlies a 1-cm-thick dark brown (7.5Y 3/4) diagenetic iron-rich crust (0–7 cm in Fig. 6). A dark grayish brown (2.5Y 4/2) clay with dispersed foraminifers that contains numerous brown (10YR 5/3) clasts of foraminifer clay occurs from 0.07 to 0.26 mbsf and appears to be a mass-flow deposit (Fig. 6). This mass-flow unit overlies

Table 1. Site 943 coring summary.

Core	Date (1994)	Time (UTC)	Depth (mbsf)	Length cored (m)	Length recovered (m)	Recovery (%)
155-943A-						
1H	May 12	0530	0.0–4.3	4.3	4.27	99.3
2H	May 12	0645	4.3–13.8	9.5	10.07	106.0
3H	May 12	0750	13.8–23.3	9.5	8.19	86.2
4H	May 12	0945	23.3–32.8	9.5	0.00	0.0
5H	May 12	1040	32.8–40.2	7.4	7.41	100.0
6X	May 12	1315	40.2–48.8	8.6	0.00	0.0
7X	May 12	1435	48.8–58.3	9.5	2.21	23.2
8X	May 12	1620	58.3–67.8	9.5	4.58	48.2
9X	May 12	1745	67.8–77.4	9.6	3.82	39.8
10X	May 12	1910	77.4–87.0	9.6	7.99	83.2
11X	May 12	2020	87.0–96.6	9.6	8.27	86.1
12X	May 12	2150	96.6–106.3	9.7	9.65	99.5
Coring totals				106.3	66.5	62.5

Note: An expanded version of this coring summary table that includes lengths and depths of sections, location of whole-round samples, and comments on sampling disturbance is included on the CD-ROM in the back pocket of this volume.

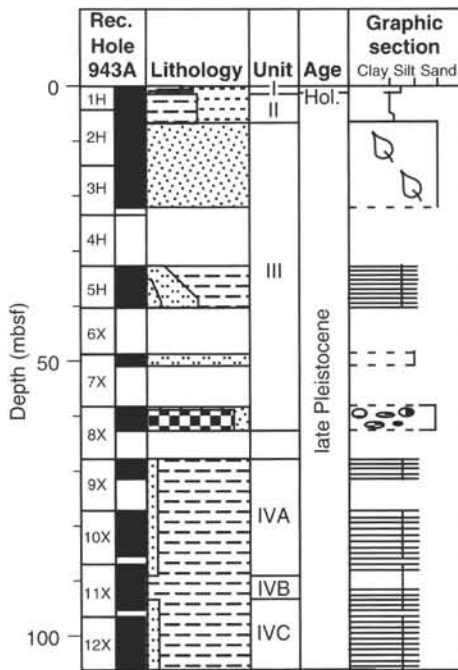


Figure 4. Composite stratigraphic section for Site 943 showing core recovery, a simplified summary of lithology, depths of unit boundaries, age, and a graphic section with generalized grain-size and bedding characteristics (simplified from Fig. 5). The lithologic symbols are explained in Figure 1 of the “Explanatory Notes” chapter, this volume. The dashed lines in the graphic section indicate that the stratigraphic extent of the sediment sequence is unknown because the upper and/or lower contact was not observed.

a dark olive gray (5Y 3/2) clay (0.26–0.82 mbsf) with mottles and contorted, deformed, and truncated laminae or color bands (Fig. 7). This clay layer contains a single centimeter-thick silt bed (interval 943A-1H-1, 39–40 cm).

At a depth of 0.81 mbsf, there is a sharp boundary between the dark olive gray clay and the underlying brown (10YR 5/3) foraminifer-nannofossil clay (Fig. 7). The carbonate content of the latter is 34.3%, and it contains a brown (7.5YR 3/4) iron-rich crust, which was recovered in the form of platy fragments 1- to 4-mm-thick and several layers with slight color banding that are similar in color to the crust. Similar crusts were analyzed previously and correlated throughout the Amazon Fan and adjacent Guiana Basin (e.g., Damuth, 1977; see “Introduction” chapter, this volume). The brown foraminifer-nannofossil clay with the iron-rich crust overlies a gray (5Y 5/1) to olive gray (5Y 5/2) nannofossil-foraminifer clay with faint burrow mottles that extends from 1.28 to 1.58 mbsf (interval 943A-1H-1, 128 cm, through -1H-2, 8 cm). The gray nannofossil-foraminifer clay has a carbonate content of 32.6%, similar to the overlying brown foraminifer-nannofossil clay. The distinct base of this interval is marked by both a color change and a band of soft nodules that probably indicates a diagenetic layer. This layer of soft nodules marks the base of Unit I, which is thicker than observed at other sites during Leg 155 because of the interbedded resedimented deposits from 0.07 to 0.82 mbsf.

Unit II

Interval: 155-943A-1H-2, 8 cm, through -2H-2, 46 cm
 Age: Holocene to late Pleistocene
 Depth: 1.58 to 6.26 mbsf

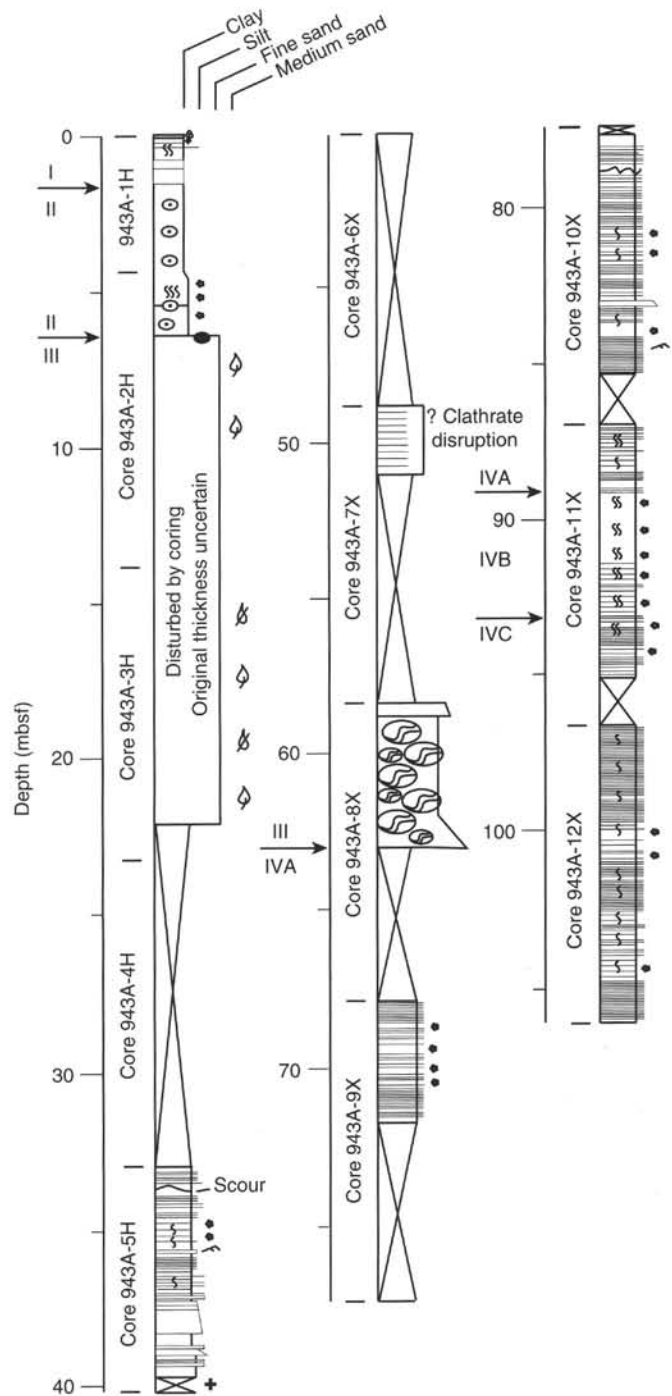


Figure 5. Graphic sedimentological columns for Site 943 showing grain-size variation (width of columns), bed thickness, and sedimentary structures; symbols and preparation of these columns are explained in the “Lithostratigraphy” section of the “Explanatory Notes” chapter, this volume. Arrows indicate the position of unit and subunit boundaries. The upper part of the column is shown in the longitudinal profile of the foldout (back pocket, this volume) to show down-fan changes in channel-fill and related mass-failure deposits.

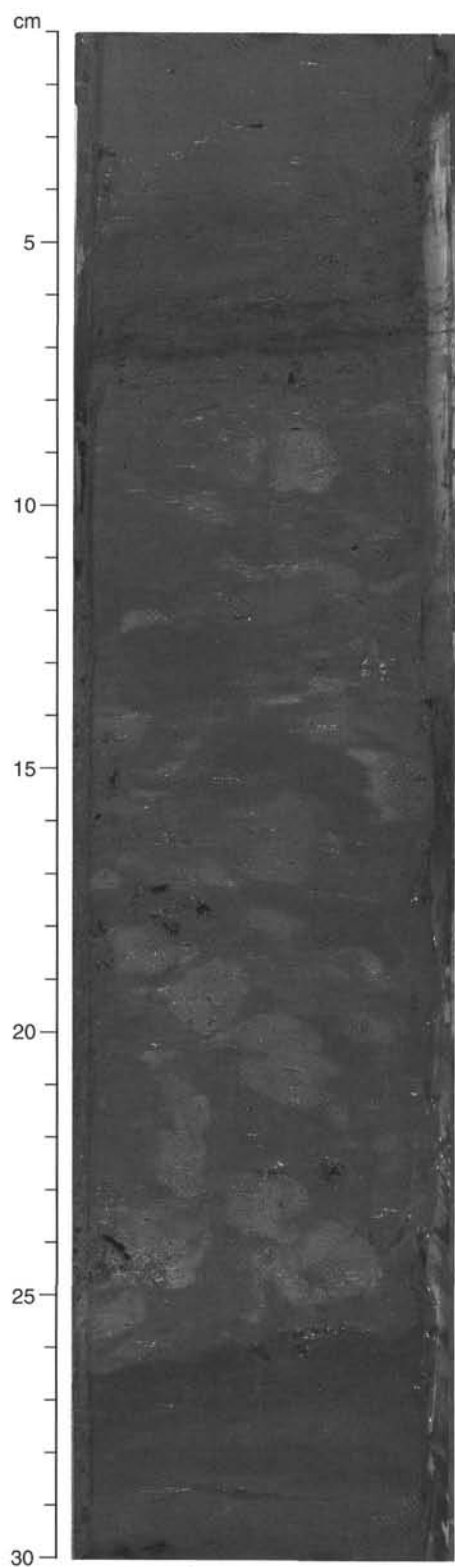


Figure 6. Mass-flow deposit containing clasts of foraminifer clay near the top of Unit I (155-943A-1H-1, 1–30 cm).

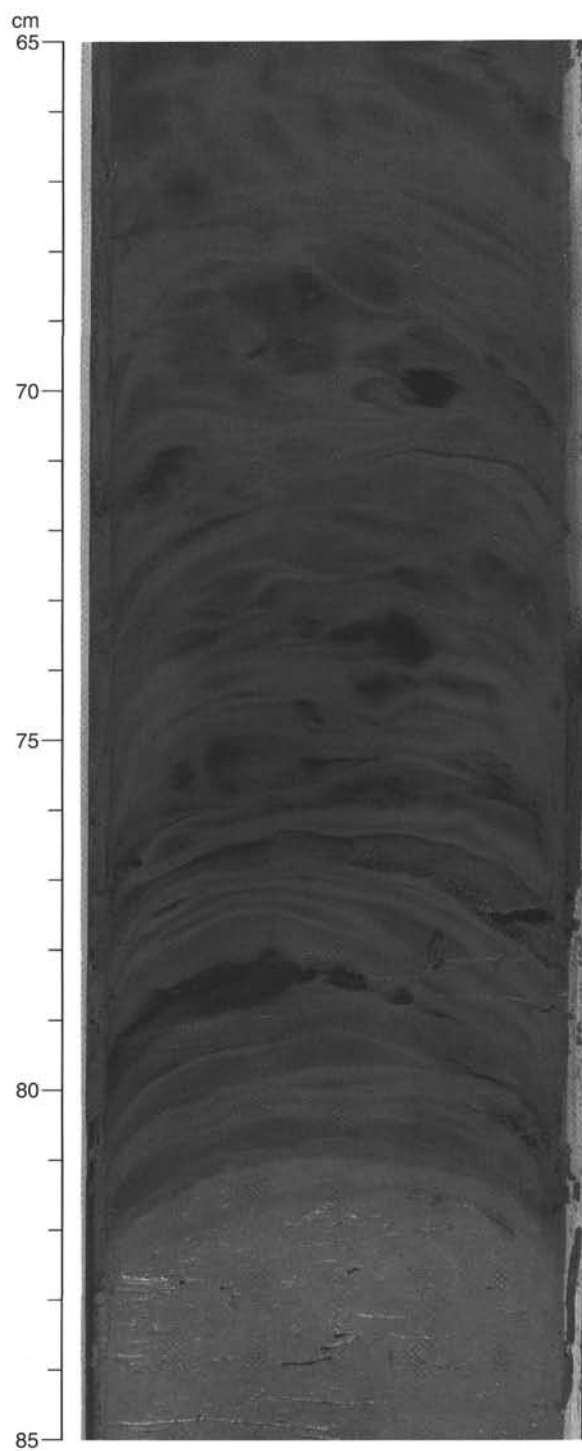


Figure 7. Basal part of mottled and color-laminated clay that underlies the mass-flow deposit shown in Figure 6 (155-943A-1H-1, 65–85 cm). The deformed and truncated laminae indicate that this is also a resedimented deposit, probably of mass-transport origin.

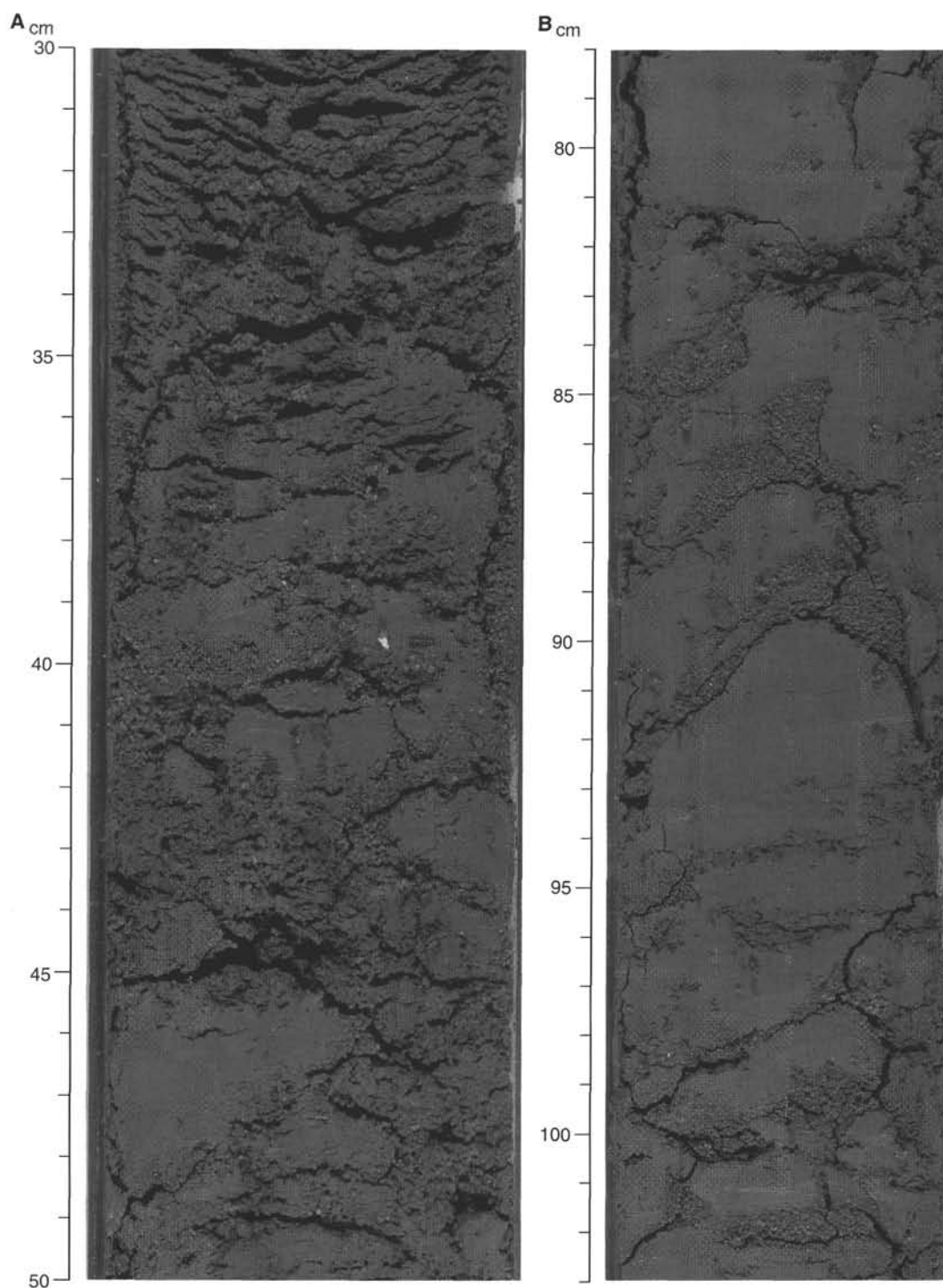


Figure 8. **A.** Base of graded sand bed (at 35 cm) overlying mud clasts in sandy matrix in lower part of Unit III (155-943A-8X-1, 30–50 cm). **B.** Mud clasts in poorly sorted sand matrix (155-943A-8X-1, 78–103 cm).

Unit II consists predominantly of interbedded clay and silty clay intervals generally with extensive burrow mottles (Figs. 4 and 5). The upper 25 cm (interval 943A-1H-2, 8–33 cm) of this unit consists of dark grayish-brown (2.5Y 4/2), massive, smooth-textured silty clay overlying a silty clay of the same color that is distinguished by a moderate abundance of black (N2/0) soft micronodules. Below about 3 mbsf, black burrow mottles and color banding generally increase downhole to the base of Unit II. The ephemeral black coloration of

the sediment is apparently from diagenetic hydrotroilite (see “Introduction” chapter, this volume). The mottled clay interval overlies a very dark gray to dark olive gray (2.5Y 3/2 to 5Y 3/2) silty clay in a transitional contact at 943A-2H-1, 8 cm (4.38 mbsf). Black hydrotroilite staining colors the sediment in layers up to 18 cm thick, and concentrations of black micronodules form laminae and beds within this silty clay interval. The base of Unit II is placed at the base of a 20-cm-thick black silty clay at 943A-2H-2, 46 cm (6.26 mbsf).

The carbonate content of Unit II was determined for the uppermost and lowermost silty clay intervals; the values were 0.8% and 2.5%, respectively.

Unit III

Interval: 155-943A-2H-2, 46 cm, through -8X-CC, 29 cm

Age: late Pleistocene

Depth: 6.26 to 62.88 mbsf

Unit III includes the coarsest grained and thickest beds recovered at this site and is the most incompletely recovered interval (only 40% of 54.9 m cored; Figs. 4 and 5). The four lithologic sequences described below represent the sediment from a single hole and are separated by 5–10 m intervals with no recovery. They do not constitute definable subunits because the only observed contact was the top of Unit III itself.

The top of the unit is marked by a large clast of gray (5Y 5/1) nanofossil-bearing clay (interval 943A-2H-2, 46–66 cm). This clast has a carbonate content of 6.3%, which is the highest value measured in Unit III. The clast rests in the top of more than 15 m of very dark gray (5Y 3/1) massive fine sand with numerous millimeter-size plant fragments. There are no original depositional structures in the sand, which appears in all sections to be highly disturbed as a result of “flow-in” during piston coring. The recovered sand extends from 6.46 to 21.99 mbsf (interval 943A-2H-2, 66 cm, through -3H-CC, 26 cm); however, the number and original thicknesses of the sand beds cannot be determined. Shell fragments (pteropods) and mica are common in the lower part of this sandy interval (e.g., Core 943A-3H). The base of the sand was not recovered, and there is a 10.61 m gap of no recovery to the next recovered section at 32.80 mbsf (Core 943A-5H, Fig. 4).

The interval from 32.80 to 40.21 mbsf (Core 943A-5H) consists of very dark gray (5Y 3/1) silty clay with numerous silt laminae and beds of silt and sand, commonly with erosive bases. There is a general trend toward thicker beds in the lower part of the recovered interval. The thickest bed is 81 cm and grades upward from clean coarse silt with large mud clasts to laminated fine silt and clayey silt. Sand and silt beds form more than 30% of this interval. An 8.69-m gap with no core recovery to 48.80 mbsf occurs between this interval and the next recovered core (Core 943A-7X).

The entire interval from 48.80 to 51.01 mbsf is very dark gray (5Y 3/1) silt with rare flattened mud clasts near the base (in Section 943A-7X-CC). Gas expansion has destroyed most sedimentary structures, and several intervals developed a bubble and honeycomb structure from escaping gas; these intervals may have contained gas hydrates.

The deepest sequence from Unit III is the interval from 58.30 to 62.88 mbsf (Core 943A-8X). A 19-cm-thick normally graded bed (very coarse sand to silt) overlies a 2-m-thick section of deformed mud and clay clasts in a fine to very coarse sand matrix (Fig. 8). “Wood-grain” structure (see “Lithostratigraphy” section in the “Explanatory Notes” chapter, this volume) was observed in the larger clasts (Fig. 9). The carbonate content of the deformed clasts is 3%. Below 60.74 mbsf (Section 943A-8X-2 at 106 cm), some of the silt laminae and silty-clay interbeds may be in place, but adjacent intervals show a high degree of deformation (i.e., “wood-grain” structure; Fig. 10). Thus the effects of XCB coring tend to obscure original depositional structure. The carbonate content of Unit III averages less than 2% when the measurements from clasts in the upper and lower intervals are excluded.

Unit IV

Interval: 155-943A-9X-1, through -12X-CC

Age: late Pleistocene

Depth: 67.80 to 106.25 mbsf

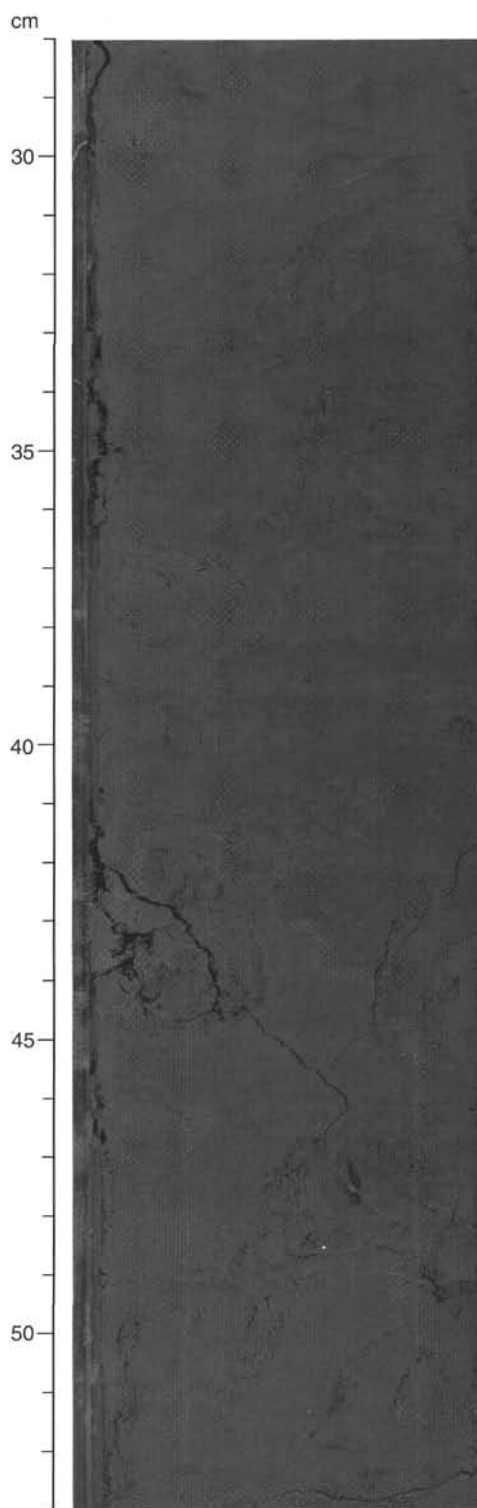


Figure 9. “Wood-grain” structure produced by internal shearing and deformation during drilling in larger mud clasts in basal part of Unit III (155-943A-8X-2, 28–53 cm).



Figure 10. Remnants of deformed sand beds and/or matrix between mud clasts in basal part of Unit III (155-943A-8X-3, 114–134 cm). Note “wood-grain” structure.

Unit IV is dominantly very dark gray (5Y 3/1) silty clay with laminae and thin beds of silt. Color banding is common in the lower part of the unit. The carbonate content of Unit IV is uniformly low, averaging 1.7% with all values less than 2.5%. Unit IV is divided into subunits based on the frequency of occurrence of common silt laminae, thin silt beds, and sandy silt beds (Figs. 4 and 5).

Subunit IVA

Subunit IVA extends from 67.80 to 89.19 mbsf (interval 943A-9X-1, 0 cm, through -11X-2, 69 cm). This subunit consists of dark gray (5Y 4/1) clay with numerous silt laminae and beds; many of the silt beds are deformed by XCB coring (Fig. 11). This subunit contains about 15 silt layers per meter; only one of the beds has fine sand at its base (Fig. 12). The deepest silt bed in this subunit is at 84.85 mbsf (Section 943-10X-6 at 11 cm) and is the base of a 6-m interval with the greatest number of silt beds/meter (5 beds/m) and the highest percentage of silt (10%) in this subunit. The base of this subunit is placed at the deepest silt lamina, which marks an abrupt change in the frequency of silt laminae.

Subunit IVB

Subunit IVB extends from 89.19 to 93.29 mbsf (interval 943A-11X-2, 69 cm, through -11X-5, 29 cm) and is characterized by very dark gray (5Y 3/1) silty clay with extensive black burrow mottles throughout. Color banding and two silt laminae are present in the lower half of this subunit.

Subunit IVC

Subunit IVC extends from the base of Subunit IVB (93.29 mbsf) to a depth of 106.25 mbsf (interval 943A-12X-5, 29 cm, through -12X-CC). This subunit consists of dark to very dark gray (5Y 4/1 to 5Y 3/1) silty clay with numerous laminae and beds of silt. The average number of laminae and beds of silt per meter is comparable to Subunit IVA (i.e., 17 laminae/m and 4.5 beds/m, respectively). Color banding extends throughout the subunit and is most noticeable in the intervals with fewer silt layers (Fig. 5).

Mineralogy

Mineralogy was determined by estimation of mineral volume percentages in smear slides and by X-ray diffraction (XRD) analysis of samples from silt layers.

Smear-slide Synthesis

The silty clays at the top of Unit II and in Unit IV are composed of 50%–75% clay; the silt fraction consists of about 70% quartz (mainly monocrystalline), 7%–12% feldspar (mainly plagioclase), 2%–7% mica, and 5%–12% accessory minerals. These units also contain 0%–3% plant debris and about 1% sponge spicules. A sample from the thick silt sequence in Unit III (Sample 943A-7X-CC, 11–12 cm) contains 10% sand, 70% silt, and 20% clay. The sand and silt composition is 70% quartz, 8% feldspar, 15% accessory minerals, and 5% mica.

XRD Data

Bulk XRD analysis was performed on seven samples of silty clay and two samples of fine sand from Cores 943A-1H through -12X (Table 2). The common minerals throughout the cored succession, based on the relative intensities of their primary peaks (normalized to quartz intensity), are quartz, plagioclase, augite, and the clay minerals smectite, illite (+ mica), and kaolinite (Figs. 13A and 13B). A few samples contain hornblende and K-feldspar. Except for differences in the content of clay minerals, the major mineral groups show little variation with depth (Fig. 13A). The low relative intensities of clay minerals at 19, 50, and 60 mbsf in Unit III (Fig. 13B) are in samples of fine sand and silt. The underlying Unit IV shows little variation in the clay-mineral content.

Spectrophotometry

Light-reflectance measurements were not obtained at this site because of the high water content of the sand in Cores 943A-2H and

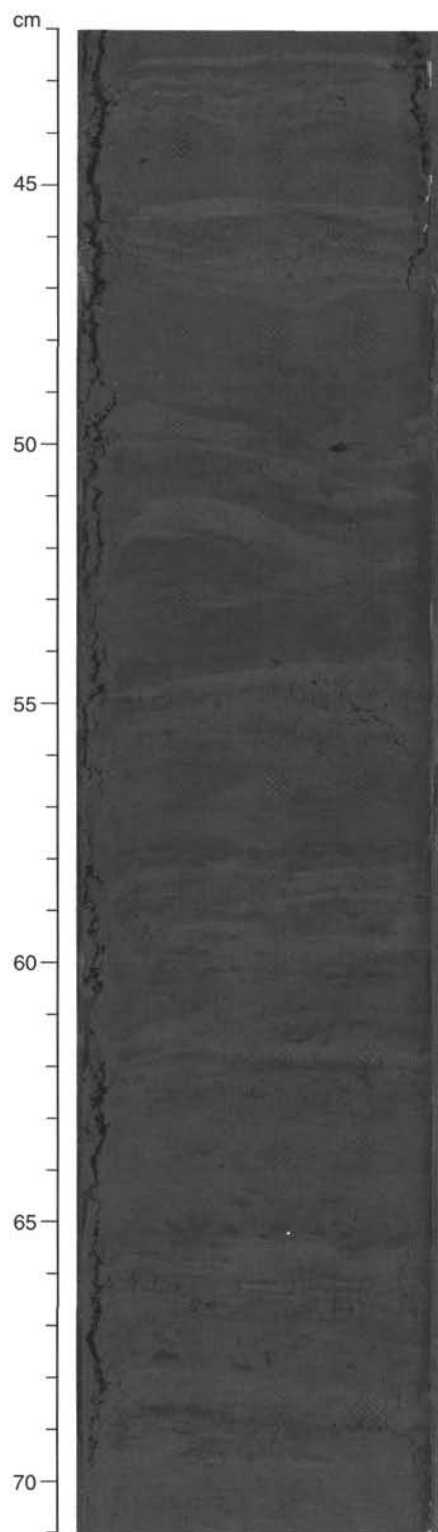


Figure 11. Laminae and beds of silt in Subunit IVA showing the anvil structure from XCB coring (155-943A-10X-4, 42–71 cm; see “Lithostratigraphy” section of “Explanatory Notes” chapter, this volume).

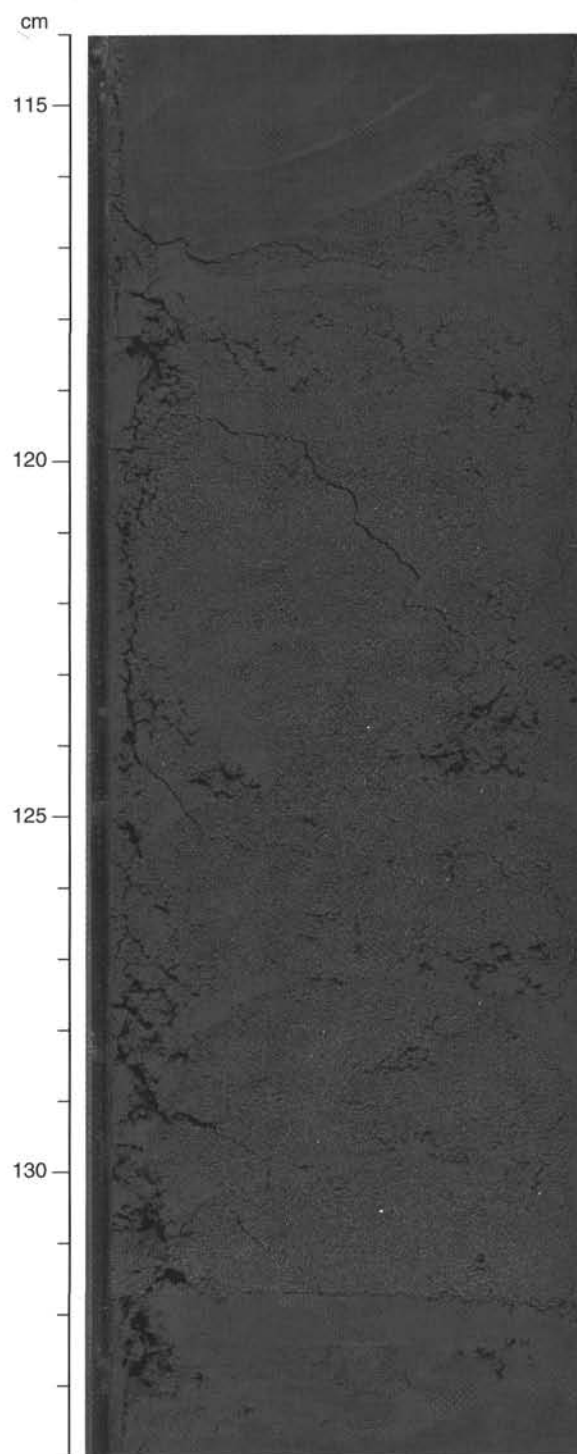


Figure 12. Slightly graded fine sand bed from Subunit IVA (155-943A-10X-4, 114–134 cm).

-3H and because of the poor recovery in the succeeding five cores (Fig. 4).

Discussion

The two most significant observations from Site 943 are: (1) the Holocene calcareous clay interval (Unit I) contains interbedded re-

Table 2. Relative peak intensities of the main minerals from representative lithologies from Site 943.

Core, section, interval (cm)	Lithology	Depth (mbsf)	Relative intensity of primary peaks							
			Smectite	Mica + Illite	Kaolinite	Quartz	Plagioclase	K-feldspar	Augite	Hornblende
155-943A-										
1H-2, 25–26	Silty clay	1.75	5.3	16.3	10.8	100.0	8.8	*	4.1	*
3H-4, 111–112	Fine sand	19.41	0.3	2.7	1.5	100.0	5.1	3.1	*	0.3
5H-2, 107–108	Silty clay	35.37	10.3	12.9	9.2	100.0	10.7	4.4	2.1	*
7X-1, 103–104	Silt	49.83	3.9	5.8	2.0	100.0	9.1	2.9	0.9	2.0
8X-2, 94–95	Fine sand	60.62	2.7	10.5	5.0	100.0	7.5	4.7	1.5	1.0
9X-2, 25–26	Silty clay	69.55	9.0	20.7	13.7	100.0	13.7	*	3.5	*
10X-1, 75–76	Silty clay	78.15	8.0	18.6	8.4	100.0	8.0	*	2.5	*
11X-4, 40–41	Silty clay	91.90	7.5	22.2	12.1	100.0	10.0	6.3	3.4	*
12X-5, 77–78	Silty clay	103.37	7.4	20.8	11.4	100.0	9.0	*	3.5	*

Notes: See "Lithostratigraphy" section in the "Explanatory Notes" chapter, this volume, for XRD methods. * = non-detection.

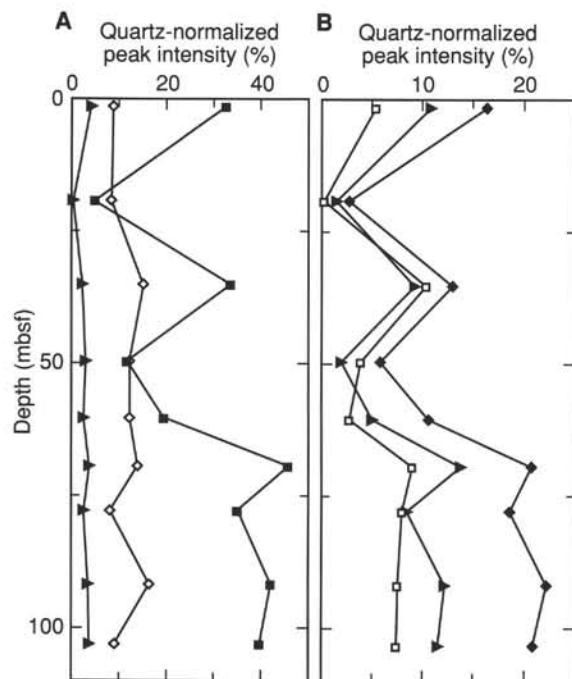


Figure 13. Relative abundances of silicate minerals in silty clay samples, based on XRD analysis. **A.** Plot against depth of the quartz-normalized peak intensities of the major mineral groups (quartz peak intensity set at 100%). Squares = clay minerals + mica; diamonds = feldspar; triangles = augite + hornblende. **B.** Plot against depth of the quartz-normalized peak intensities of clay minerals and micas. Squares = smectite; diamonds = mica + illite; triangles = kaolinite. See text for discussion.

sedimented units, probably mass transport deposits; and (2) the channel-fill sequence, Unit III, extends only to 67.80 mbsf, whereas the deeper section consists of levee deposits, probably of two different systems or episodes of deposition (Subunits IVA and IVC).

The debris-flow unit with carbonate mud clasts, the silt bed (probably turbidite deposit), and the underlying laminated clays in Unit I indicate that some terrigenous sediment transport occurred in the main Amazon Channel after sea level in the Holocene rise cut off the continuous supply of terrigenous sediment. The source for these re-sedimented deposits is uncertain but might have been either from the continental margin or a localized slump within the channel up-fan. These deposits were not recovered in the adjacent levee (Site 944), indicating that they were the result of thin flows that mostly remained confined to the channel itself.

The sinuous nature of the channels on the Amazon Fan implies lateral migration is common during at least their early development.

The 60-m-thick interval of coarse-grained deposits that compose Unit III suggests that the channel reached this site relatively soon after migration of levee growth either by lateral or down-fan migration or progradation. The depositional events that mark initiation of channel activity are not known because the basal contact of the channel facies was not recovered. The deepest recovered sediment consists of angular mud clasts in a coarse sand matrix; this deposit would be consistent with erosion of fan sediment, either locally or upstream, during migration of the channel to the area. The overlying silt and sand sequences would be the aggradational part of the channel fill. The channel-fill sediment overlies typical Amazon Fan levee deposits. The upper levee sequence, Subunit IVA, may be related to the Amazon Channel. The lower levee sequence, Subunit IVC, has subtle differences both in the silt units (such as better sorting) and the texture of the interbedded silty clays, compared to Subunit IVA; these differences suggest that Subunit IVC may be related to an older channel system, probably the Purple Channel-levee System (see "Core-Seismic Integration" section, this chapter).

BIOSTRATIGRAPHY

Calcareous Nannofossils

All calcareous nannofossils recovered at Site 943 are from nannofossil Zone CN15b (Table 3). An abundant and well-preserved nannofossil assemblage with low diversity is present in the calcareous nannofossil and foraminifer clay in the mud-line sample. Nannofossils are absent from the mass-flow deposit, from 0.14 to 0.77 mbsf, and reappear in high abundance below this interval in the calcareous clay of Unit I (Table 3). Nannofossils are rare or absent in Unit II to IV of Hole 943A (Samples 943A-1H-CC, 3–12 cm, through -12X-CC, 55–64 cm). In Unit IV, lighter colored intervals (943A-11X) are barren of nannofossils, but contain carbonate particles (siderite) as was observed in the deeper part of Site 942.

Planktonic Foraminifers

The boundary between Ericson Zones Z and Y is at the top of Unit II, between 1.64 and 2.70 mbsf (Samples 943A-1H-2, 14–16 cm, and -1H-2, 120–122 cm; Table 4; Fig. 14). The position of the Z/Y boundary is complicated by the absence of *G. tumida* and *G. menardii* in the mass-flow deposit from 0.33 to 0.79 mbsf. Planktonic foraminifers are absent in Unit III between 14.2 and 62.8 mbsf (Samples 943A-2H-CC, 22–31 cm, through -8H-CC, 19–28 cm). Rare planktonic foraminifers are found in Unit IV. The absence of *P. obliquiloculata* in Unit IV suggests that this unit could be younger than 40 ka.

Benthic Foraminifers

Benthic foraminifers are rare or absent in Hole 943A.

Table 3. Calcareous nannofossil and siliceous microfossil abundance data for Hole 943A.

Core, section, interval (cm)	Top interval (mbsf)	Bottom interval (mbsf)	Calcareous nannofossils			Diatoms		Sponge spicules	Radiolarians	Ericson Zone (inferred from foraminifers)	Age (inferred from foraminifers)
			Abundance	Preservation	Zone	Marine	Fresh water				
155-943A-											
1H-MI, 0-0	0.00	0.00	a	ne	CN15b	r	r	—	—	Z	Holocene
1H-1, 5-7	0.05	0.07	a	ne		—	—	—	—	Z	Holocene
1H-1, 7-9	0.07	0.09	a	ne		—	—	—	—	Z	Holocene
1H-1, 10-12	0.10	0.12	a	ne		—	—	—	—	Z	Holocene
1H-1, 14-16	0.14	0.16	b	—		—	—	—	—	Z	Holocene
1H-1, 33-35	0.33	0.35	tr	—		—	—	—	—	Z	Holocene
1H-1, 50-52	0.50	0.52	tr	—		—	—	—	—	Z	Holocene
1H-1, 77-79	0.77	0.79	vr	—		—	—	—	—	Z	Holocene
1H-1, 85-87	0.85	0.87	a	ne		—	—	—	—	Z	Holocene
1H-1, 110-112	1.10	1.12	a	ne		—	—	—	—	Z	Holocene
1H-1, 120-122	1.20	1.22	vr	—		—	—	—	—	Z	Holocene
1H-1, 136-138	1.36	1.38	a	ne		—	—	—	—	Z	Holocene
1H-CC, 3-12	4.20	4.29	tr	—		—	—	—	—	Y	late Pleist.
2H-CC, 22-31	14.20	14.29	b	—		—	—	—	—	Y	late Pleist.
5H-CC, 16-25	21.89	21.98	b	—		—	—	—	—	Y	late Pleist.
7X-CC, 0-1	32.79	32.80	b	—		—	—	—	—	Y	late Pleist.
8X-CC, 21-30	40.11	40.20	b	—		—	—	—	—	Y	late Pleist.
9X-CC, 22-31	50.91	51.00	b	—		—	—	—	—	Y	late Pleist.
10X-CC, 19-28	62.78	62.87	b	—		—	—	—	—	Y	late Pleist.
11X-1, 22-31	71.52	71.61	tr	—		—	—	—	—	Y	late Pleist.
11X-1, 27-36	85.29	85.38	tr	—		—	—	—	—	Y	late Pleist.
11X-2, 122-122	89.72	89.72	b	—		—	—	—	—	Y	late Pleist.
11X-4, 48-48	91.98	91.98	vr	—		—	—	—	—	Y	late Pleist.
11X-5, 62-62	93.62	93.62	tr	—		—	—	—	—	Y	late Pleist.
11X-CC, 33-42	95.17	95.26	tr	—		—	—	—	—	Y	late Pleist.
12X-CC, 55-64	106.15	106.24	vr	—		—	—	—	—	Y	late Pleist.

Siliceous Microfossils

Hole 943A is barren of diatoms, except for the mud-line sample, where marine and freshwater diatoms occur in low abundance (Table 4).

Palynology

Four samples were examined from Hole 943A (Table 5). Pollen and spore assemblages were obtained from clay, silty clay, and silt in Units II, III, and IV between 5.29 and 176.84 mbsf (Fig. 14). Present in the assemblages are *Byrsonima*, Gramineae, *Cassia*, and Cyperaceae pollen with Cyathaceae and monolete spores. This is similar to late-Pleistocene-age pollen and spore assemblages obtained at previous sites (e.g., Site 940). Wood particles were observed in moderate abundance in all four samples. Macroscopic wood fragments (>63 µm) were observed in core-catcher samples at 40.11, 62.78, and 71.52 mbsf. Dinoflagellates were not found.

Stratigraphic Summary

Unit I contains nannofossil and planktonic foraminifer assemblages indicative of the Holocene. The nannofossil assemblages are well preserved and represent nannofossil Zone CN15b. The boundary between Ericson Zones Z and Y is at the top of Unit II, between 1.64 and 2.70 mbsf. Unit III is barren of foraminifers and nannofossils. The absence of *P. obliquiloculata* in Unit IV suggests that this unit could be younger than 40 ka.

PALEOMAGNETISM

Remanence Studies

Measurements of archive-half sections from five APC cores and six XCB cores of Hole 943A were made on the pass-through cryogenic magnetometer. Cores 943A-3H and -5H were azimuthally oriented with the Tensor tool.

Oscillations in declination, inclination, and remanence intensity, which we interpret as secular variation, were observed in Core 943A-

1H from 0 to 4 mbsf (Fig. 15) and in Core 943A-5H from 34 to 37 mbsf (Fig. 16). Two presumed cycles of secular variation within a dark gray clay (mass flow?) from 0.14 to 0.77 mbsf are observed in Core 943A-1H. This gray clay is surrounded by brown Holocene calcareous clay (see "Biostratigraphy" section, this chapter) with an associated iron-rich crust above (0.06-0.07 mbsf) and below (1.09-1.15 mbsf) it, and could represent a repeat section resulting from a small slump. Apparent secular variation cycles again appear at ~1.6 mbsf with the gray clay of Unit II (Fig. 15). Flow-in at the bottom of Core 943A-1H begins to distort the remanence intensity signal at 3 m. The interval from 34 to 37 mbsf in Core 943A-5H is composed of silty clay of late Pleistocene age and contains eight oscillations.

Remanence intensity, after AF demagnetization to 20 mT, displayed large variations with depth. The data suggest two intensity peaks at ~5 m and ~35 m, with a possible third peak at ~97 m (Fig. 17). These peaks may correspond to remanence intensity peaks that occurred in the Amazon Channel deposits of Holes 935A, 939B, and 940A. However, the poor recovery in the top 60 m of Hole 943A makes this correlation tenuous. No geomagnetic excursions were observed in the sediment recovered from Hole 943A.

Magnetic Susceptibility Studies

Whole-core magnetic and discrete-sample susceptibilities were measured on all cores collected from Site 943. Both data sets show similar trends downhole (Fig. 18). Unit III contains the highest susceptibility values for the site. In particular, the values are highest within the sand. This contrasts with the low susceptibility values of Site 935 sand. The difference may reflect poor sorting at this site. The lowest susceptibility values are found within Unit I.

ORGANIC GEOCHEMISTRY

Volatile Hydrocarbons

Headspace methane concentrations increase rapidly below the sediment surface to 9500 ppm at 5.80 mbsf (Table 6; Fig. 19). Methane concentrations remain fairly constant below this depth, ranging from 5500 ppm at 38.80 mbsf to 12,900 ppm at 91.50 mbsf. The two

Table 4. Foraminifer abundance data for Hole 943A.

Core, section, interval (cm)	Top interval (mbsf)	Bottom interval (mbsf)	<i>Globorotalia menardii</i>	<i>Globorotalia tumida</i>	<i>Globorotalia tumida flexuosa</i>	<i>Pulleniatina obliquiloculata</i>	<i>Globigerinoides ruber</i> (white)	<i>Globigerinoides ruber</i> (pink)	<i>Globorotalia hexagonus</i>	<i>Neogobolobadrina duterrei</i>	<i>Globorotalia trilobus trilobus</i>	<i>Globorotalia inflata</i>	<i>Globorotalia truncatulinoides</i>	<i>Globigerina bulloides</i>	<i>Globigerinoides trilobus sacculifer</i>	<i>Globorotalia fimbriata</i>	<i>Bolliella adamsi</i>	<i>Hasigerinella digitata</i>	<i>Globigerina calida calida</i>	<i>Globorotalia crassaformis hessi</i>	<i>Globorotalia crassaformis viola</i>	<i>Globorotalia tosaensis</i>	<i>Globorotalia crassaformis crassaformis</i>	Other planktonic foraminifers	Vivianite nodules	Overall foraminifer abundance	Preservation	Abundance of bathyal benthic foraminifers	Abundance of abyssal benthic foraminifers	Comments	Ericson Zone	Age			
155-943A-																																			
1H-1, 5-7	0.05	0.07	C	F	B	F	C	F	B	C	B	B	B	C	B	B	B	B	B	B	B	B	B	B	B	A	G	B	B	S		Z	Holocene		
1H-1, 10-12	0.1	0.12	C	F	B	R	C	F	B	C	F	B	B	F	B	B	B	B	B	B	B	B	B	B	B	C	G	B	B			Z	Holocene		
1H-1, 33-35	0.33	0.35	B	B	B	B	B	B	B	B	B	B	B	B	B	B	B	B	B	B	B	B	B	B	B	B	B	B	B			Z	Holocene		
1H-1, 50-52	0.5	0.52	R	B	B	R	C	B	B	F	C	B	F	B	B	B	B	B	B	B	B	B	B	B	B	R	G	B	B	M		Z	Holocene		
1H-1, 77-79	0.77	0.79	B	B	B	B	B	B	B	B	B	B	B	B	B	B	B	B	B	B	B	B	B	B	B	B	B	B	B			Z	Holocene		
1H-1, 85-87	0.85	0.87	C	F	B	R	C	R	B	C	C	B	F	B	F	B	B	B	B	B	B	B	B	B	B	A	G	B	R			Z	Holocene		
1H-1, 110-112	1.1	1.12	C	R	B	R	C	R	B	C	C	B	B	B	F	B	B	B	B	B	B	B	B	B	B	A	G	B	B			Z	Holocene		
1H-1, 136-138	1.36	1.38	R	C	B	B	C	R	B	C	C	B	B	B	F	B	B	B	B	B	B	B	B	B	B	A	G	B	B			Z	Holocene		
1H-2, 5-7	1.55	1.57	B	C	B	F	C	R	B	C	C	B	F	B	F	B	B	B	B	B	B	B	B	B	B	C	G	B	B			Z	Holocene		
1H-2, 14-16	1.64	1.67	B	R	B	R	R	R	B	R	B	B	B	B	B	B	B	B	B	B	B	B	B	B	B	B	M	B	B			Z	Holocene		
1H-2, 120-122	2.70	2.72	B	B	B	C	F	B	B	C	C	B	B	B	C	B	B	B	B	B	B	B	B	B	B	C	G	B	B			Y	late Pleist.		
1H-CC, 3-12	4.20	4.29	C	C	B	R	F	F	B	C	F	B	B	B	F	B	B	B	B	B	B	B	B	B	B	A	G	B	B			Y	late Pleist.		
2H-CC, 22-31	14.20	14.29	B	B	B	B	B	B	B	B	B	B	B	B	B	B	B	B	B	B	B	B	B	B	B	B	B	B	B	S			Y	late Pleist.	
3H-CC, 16-25	21.89	21.98	B	B	B	B	B	B	B	B	B	B	B	B	B	B	B	B	B	B	B	B	B	B	B	B	B	B	B	S			Y	late Pleist.	
4H-CC, 0-1	32.79	32.80	B	B	B	B	B	B	B	B	B	B	B	B	B	B	B	B	B	B	B	B	B	B	B	C	B	B	B	S,M			Y	late Pleist.	
5H-CC, 21-30	40.11	40.20	B	B	B	B	B	B	B	B	B	B	B	B	B	B	B	B	B	B	B	B	B	B	B	B	B	B	B	M,W			Y	late Pleist.	
7X-CC, 22-31	50.91	51.00	B	B	B	B	B	B	B	B	B	B	B	B	B	B	B	B	B	B	B	B	B	B	B	B	B	B	B	S			Y	late Pleist.	
8X-CC, 19-28	62.78	62.87	B	B	B	B	B	B	B	B	B	B	B	B	B	B	B	B	B	B	B	B	B	B	B	B	B	B	B	S,W,M			Y	late Pleist.	
9X-CC, 22-31	71.52	71.61	B	B	B	B	F	B	B	C	C	B	B	B	C	B	B	B	B	B	B	B	B	B	B	A	R	G	B	S,W,M			Y	late Pleist.	
10X-CC, 27-36	85.29	85.38	B	B	B	B	B	C	B	C	C	B	B	B	B	B	B	B	B	B	B	B	B	B	B	A	R	M	R	B	M			Y	late Pleist.
11X-CC, 33-42	95.17	95.26	B	B	B	B	B	B	B	B	B	B	B	B	B	B	B	B	B	B	B	B	B	B	B	A	B	B	B	S,M			Y	late Pleist.	
12X-CC, 55-64	106.15	106.24	B	B	B	B	R	B	B	B	R	B	B	B	R	B	B	B	B	B	B	B	B	B	B	R	R	B	B	M,BN			Y	late Pleist.	

Notes: Key to Comments section: Sediment composition: S = sand, M = mica, BN = black nodules; indicators of reworking: W = wood fragments.

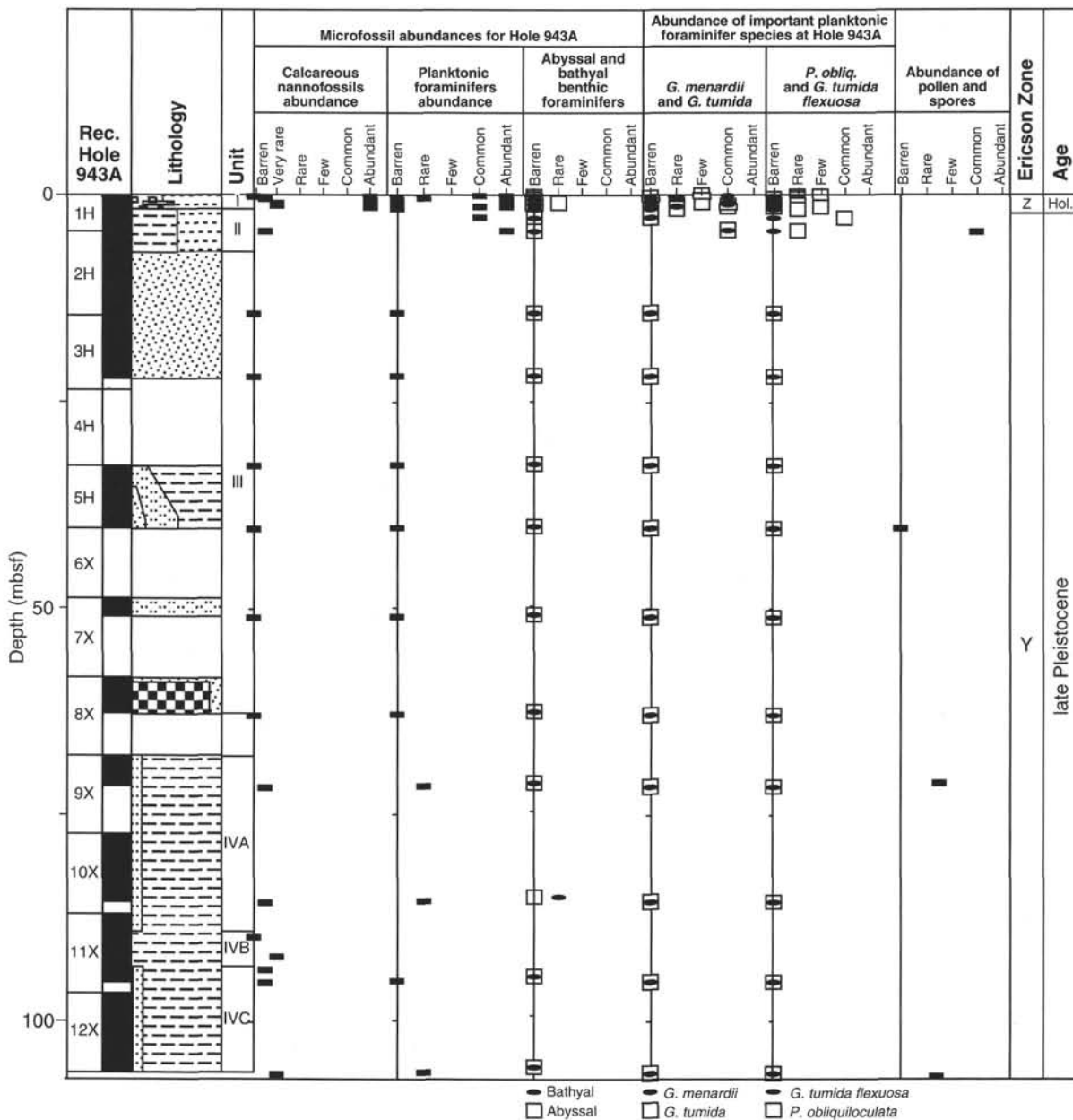


Figure 14. Biostratigraphic summary for Site 943.

Table 5. Spores and pollen data for Hole 943A.

Core, section, interval (cm)	Top interval (mbsf)	Bottom interval (mbsf)	Pollen and spores			Dinocysts	Wood/ carbonized particles	Ericson Zone (inferred from forams.)	Age (inferred from forams.)
			Abundance	Preservation	Major types recorded				
155-943A-									
1H-CC, 12-13	4.29	4.30	c	m	<i>Byrsonima</i> , Cyathaceae, monolete spore	b	f	Y	late Pleist.
5H-CC, 30-31	40.20	40.21	b	—		b	r	Y	late Pleist.
9X-CC, 31-32	71.61	71.62	f	m	Gramineae, monolete spore, <i>Cassia</i>	b	f	Y	late Pleist.
12X-CC, 64-65	106.24	106.25	r	p	Cyperaceae	b	f	Y	late Pleist.

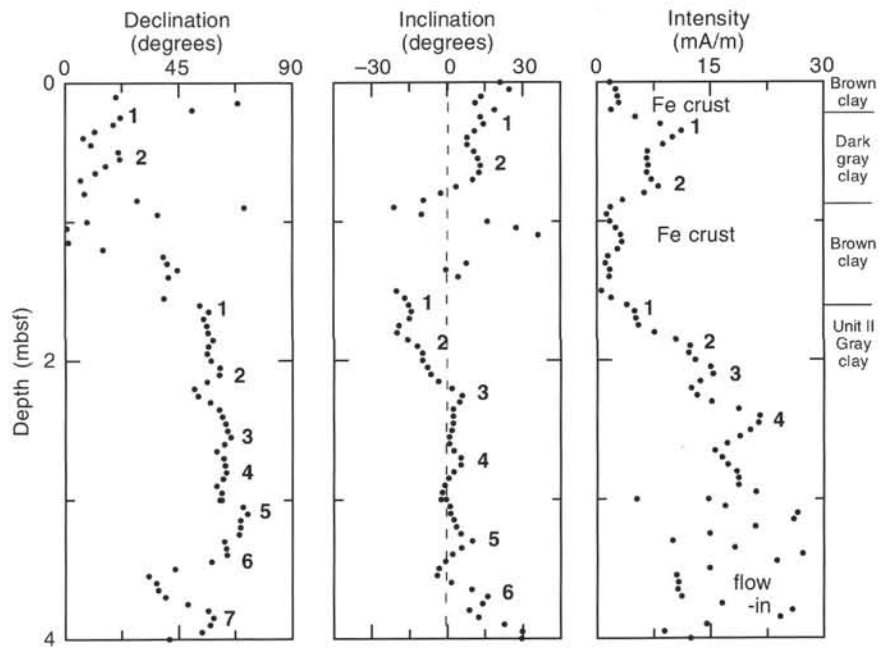


Figure 15. Uncorrected declination, inclination, and remanence intensity, after AF demagnetization to 20 mT, for the interval 0–4 mbsf in Hole 943A. Positions of two iron- (Fe) rich crusts within the brown calcareous clays are indicated. Oscillation peaks, interpreted as secular variation cycles, are numbered 1–2 in the upper gray clay (0.14–0.77 mbsf) and 1–7 in the lower gray clay (below 1.6 m). Flow-in zone at the bottom of the interval is indicated on the intensity plot.

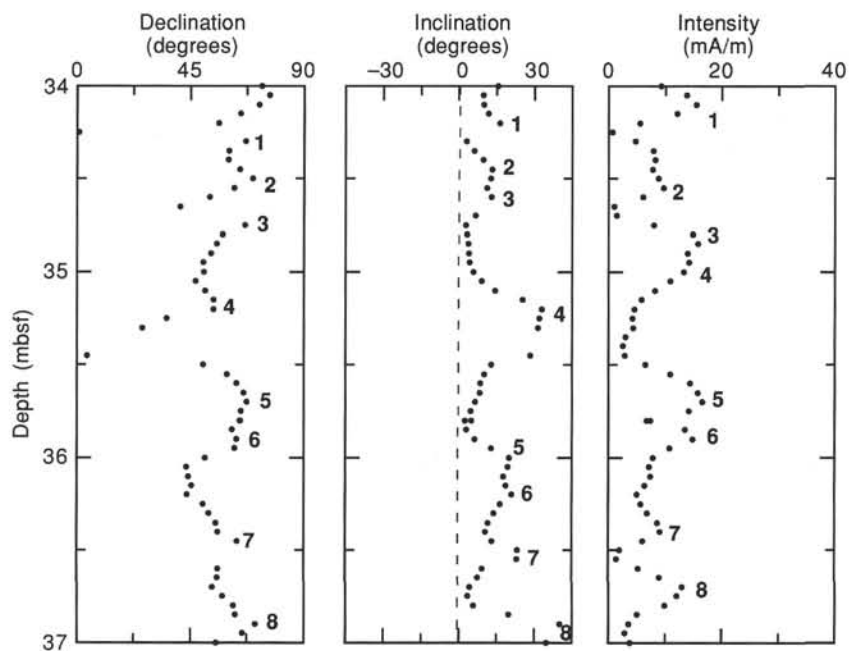


Figure 16. Azimuthally corrected declination, inclination, and remanence intensity, after AF demagnetization to 20 mT, for the interval 34–37 mbsf in Hole 943A. Oscillation peaks, interpreted as secular variation, are numbered 1–8.

vacutainer methane values obtained at 38.80 (504,000 ppm) and 61.18 mbsf (46,500 ppm) are considerably higher than headspace concentrations. Higher molecular weight hydrocarbons were not found, indicating a predominantly biogenic methane source at Site 943.

Carbon, Nitrogen, and Sulfur Concentrations

High carbonate (calculated as CaCO₃) contents are found at 0.04 mbsf (10%), 0.92 mbsf (34%), and 1.40 mbsf (32%), corresponding to Holocene sediment (Table 7; Fig. 20). Another elevated value (6.3%) was measured in a nannofossil-bearing clay clast at 6.33 mbsf. The rest of Hole 943A displays low carbonate concentrations

(0.6% to 3%). TOC is less than 0.4% in the top 1.40 mbsf and shows a relatively high value of 1.4% at 1.71 mbsf, corresponding to a short interval of olive gray clay. The TOC values in the rest of Hole 943A range from ~0.5% to ~1.1% with low values corresponding to increasing grain size. An exception is a very low concentration (0.03%) measured in a fine sand layer at 19.43 mbsf.

Total nitrogen concentrations show a profile similar to that of TOC with low values (0.05%) in the top 1.40 mbsf, a maximum value of 0.12% at 1.71 mbsf, and a very low value (0.01%) in the fine sand layer at 19.43 mbsf. In the other samples, TN concentrations range from 0.05% to 0.11%. Total sulfur concentrations, which are low throughout most of Hole 943A, are relatively high (0.8%) at 6.06 mbsf.

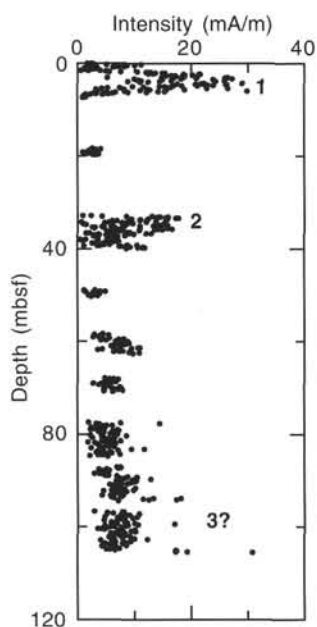


Figure 17. Remanence intensity, after AF demagnetization to 20 mT, for Hole 943A. Possible intensity peaks, which may correlate with similar peaks in Holes 935A, 939B, and 940A, are numbered 1–3.

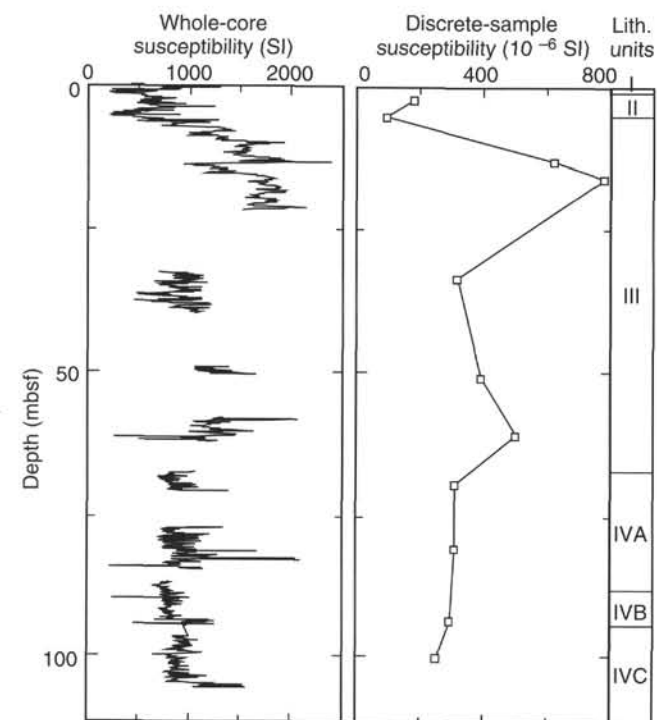


Figure 18. Whole-core and discrete-sample magnetic susceptibilities for Site 943.

The high carbonate content and low TOC and TN observed in the top 0.5 mbsf are characteristic of Holocene sediment (Unit I) throughout previous Leg 155 sites. The high sulfur value observed below the carbonate-rich Unit I is also similar to those of previous sites. The major variations in TOC and TN concentrations are associated with changes in grain size.

Table 6. Gas concentrations in sediments from Site 943.

Core, section, interval (cm)	Depth (mbsf)	Sed. temp.* (°C)	Methane	
			HS (ppm)	VAC (ppm)
155-943A-				
1H-2, 0–5	1.50	2	28	
2H-2, 0–5	5.80	2	9,456	
5H-5, 0–5	38.80	3	5,530	503,821
7X-5, 0–5	48.80	4	11,644	
8X-3, 0–5	61.18	4	7,266	46,471
9X-2, 0–5	69.30	4	8,556	
10X-4, 0–5	81.90	5	5,955	
11X-4, 0–5	91.50	5	12,871	
12X-6, 0–5	104.10	5	9,390	

Notes: HS = headspace; VAC = vacutainer. *Assumed geothermal gradient = 32°C/km. Bottom-water temperature = 2°C.

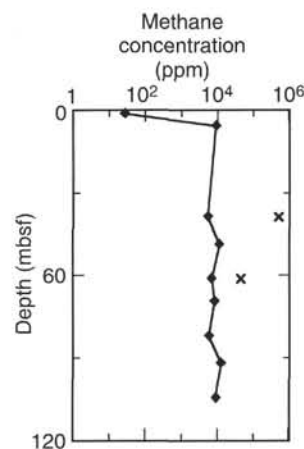


Figure 19. Methane concentrations at Site 943. Headspace (diamond) and vacutainer (x) samples are plotted.

INORGANIC GEOCHEMISTRY

Interstitial Water Analysis

Interstitial water samples were collected from five sediment samples from Hole 943A. Samples were taken at 1.45 and 7.25 mbsf and approximately every 30 m thereafter to a depth of 91.40 mbsf (Table 8; Fig. 21).

Salinities of the water samples range from 32.5 to 34.5 (Fig. 21A). The salinity decreases from 34.5 at 1.45 mbsf to 32.5 at 38.70 mbsf, and remains at 32.5 downhole.

Chloride concentrations rise from 551 at 1.45 mbsf to 560 mM at 38.70 mbsf (Fig. 21B). The values are then relatively constant through 61.08 mbsf and decrease to 556 near the bottom of the hole.

Pore-water pH ranges from 7.25 to 7.71 (Fig. 21C). The pH rises from 7.31 at 1.45 mbsf to 7.71 at 7.25 mbsf, then decreases to 7.25 near the bottom of the hole.

Pore-water alkalinity increases quickly from 8.83 mM at 1.45 mbsf to 23.80 at 7.25 mbsf and then decreases to 9.85 mM at 38.70 mbsf. Below 38.70 mbsf, alkalinity remains between 8.06 and 6.91 mM.

Dissolved magnesium and calcium concentrations decrease over the upper 7.25 mbsf; values fall from seawater concentrations to 43.3 and 7.0 mM, respectively (Figs. 21E and 21F). Below 7.25 mbsf, the values are more constant, with around 42 mM magnesium and 5 mM calcium downhole.

Pore-water sulfate concentrations decrease from 21.3 mM at 1.45 mbsf to zero by 7.25 mbsf. The values remain near zero downhole, with 1.8 mM measured at 91.40 mbsf (Fig. 21G).

Table 7. Elemental and organic carbon compositions of sediments from Site 943.

Core, section, interval (cm)	Depth (mbsf)	IC (%)	CaCO ₃ * (%)	TC (%)	TOC (%)	TN (%)	TS (%)	[C/N]a
155-943A-								
1H-1, 4-5	0.04	1.25	10.4	1.63	0.38	0.05	0.12	9
1H-1, 92-93	0.92	4.12	34.3	4.39	0.27	0.05	0.07	6
1H-1, 140-141	1.40	3.91	32.6	4.13	0.22	0.05	0.00	5
1H-2, 21-22	1.71	0.10	0.8	1.50	1.40	0.12	0.26	14
2H-2, 29-30	6.06	0.30	2.5	0.91	0.61	0.07	0.77	11
2H-2, 53-54	6.33	0.76	6.3	1.25	0.49	0.07	0.07	8
3H-4, 113-114	19.43	0.07	0.6	0.10	0.03	0.01	0.00	3
5H-1, 31-32	33.11	0.25	2.1	1.17	0.92	0.10	0.08	11
7X-1, 62-53	49.42	0.17	1.4	0.93	0.76	0.06	0.00	16
8X-2, 56-57	60.24	0.36	3.0	1.12	0.76	0.09	0.00	10
9X-1, 64-65	68.44	0.24	2.0	1.06	0.82	0.10	0.04	10
10X-3, 104-105	81.44	0.22	1.8	1.28	1.06	0.11	0.00	11
10X-3, 107-108	81.47	0.16	1.3	0.65	0.49	0.05	0.06	13
11X-4, 60-61	92.10	0.12	1.0	0.86	0.74	0.10	0.03	8
12X-5, 120-121	103.80	0.29	2.4	1.19	0.90	0.10	0.00	11

Note: * = calculated assuming all IC is calcite.

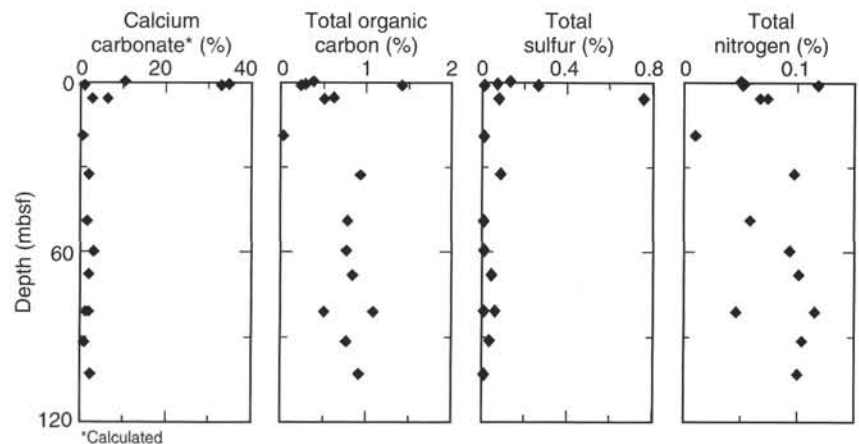


Figure 20. Concentration profiles of carbonate, total organic carbon, total sulfur, and total nitrogen in Hole 943A.

Table 8. Interstitial water chemistry, Site 943.

Core, section, interval (cm)	Depth (mbsf)	Salinity	pH	Alkalinity (mM)	Cl ⁻ (mM)	Mg ²⁺ (mM)	Ca ²⁺ (mM)	K ⁺ (mM)	HPO ₄ ²⁻ (μM)	SO ₄ ²⁻ (mM)	NH ₄ ⁺ (mM)	H ₄ SiO ₄ (μM)	Na ⁺ (mM)	Fe ²⁺ (μM)	Mn ²⁺ (μM)
155-943A-															
1H-1, 145-150	1.45	34.5	7.31	8.83	551	50.8	9.5	11.8	34.1	21.3	0.5	268	470	30.0	104.8
2H-2, 145-150	7.25	33.5	7.71	23.80	553	43.3	7.0	10.2	368.0	0.1	1.1	429	466	10.9	11.2
5H-4, 140-150	38.70	32.5	7.51	9.85	560	43.8	5.0	7.0	1.8	0.2	8.4	401	457	74.2	4.8
8X-2, 140-150	61.08	32.5	7.55	8.06	561	41.8	5.1	8.6	3.6	0.9	7.1	272	461	40.7	4.8
11X-3, 140-150	91.40	32.5	7.25	6.91	556	42.6	5.9	7.8	1.6	1.8	6.3	305	456	139.8	11.2

Ammonium concentrations increase with depth from 0.5 mM at 1.45 mbsf to 8.4 mM at 38.70 mbsf (Fig. 21H). Below 38.70 mbsf, the ammonium concentration decreases slightly to 6.3 mM at 91.40 mbsf.

Pore-water phosphate concentrations increase from 34.1 μM at 1.45 mbsf to a peak of 368 μM at 7.25 mbsf (Fig. 21I). Below 7.25 mbsf, phosphate concentrations are below 5 μM.

Dissolved silica concentrations vary from 278 to 429 μM, with no clear downhole trend (Fig. 21J).

Dissolved potassium and sodium concentrations show parallel concentration changes downhole. The concentrations decrease from 11.8 mM potassium and 470 mM sodium at 1.45 mbsf to 7.0 mM potassium and 457 mM sodium at 38.70 mbsf (Figs. 21K and 21L). Thereafter, the concentrations are relatively constant.

Dissolved iron concentrations generally increase downhole, from 10 to 30 μM in the two shallowest samples to 140 μM at 91.40 mbsf (Fig. 21M).

Manganese concentrations are quite high in the shallowest sample, 104.8 μM at 1.45 mbsf. Below 1.45 mbsf, the concentrations are between 4.8 and 11.2 μM (Fig. 21N).

PHYSICAL PROPERTIES

Index Properties

Index properties were determined for undisturbed, predominantly clayey sediment in the intervals between 2.12 and 6.38 mbsf, 33.64 and 38.99 mbsf, and 60.90 and 104.7 mbsf in Hole 943A (Table 9). Only grain density was determined for sandy sediment.

Water content is 50% in the silty clay at 2.12 mbsf, the shallowest depth sampled (Fig. 22). It increases to 59% at 3.87 mbsf and then decreases downhole to 31% at 33.64 mbsf. Below 33 mbsf, water content decreases gradually with depth to 28% at 104.70 mbsf. Between 33 mbsf and the base of Hole 943A, water content fluctuations are

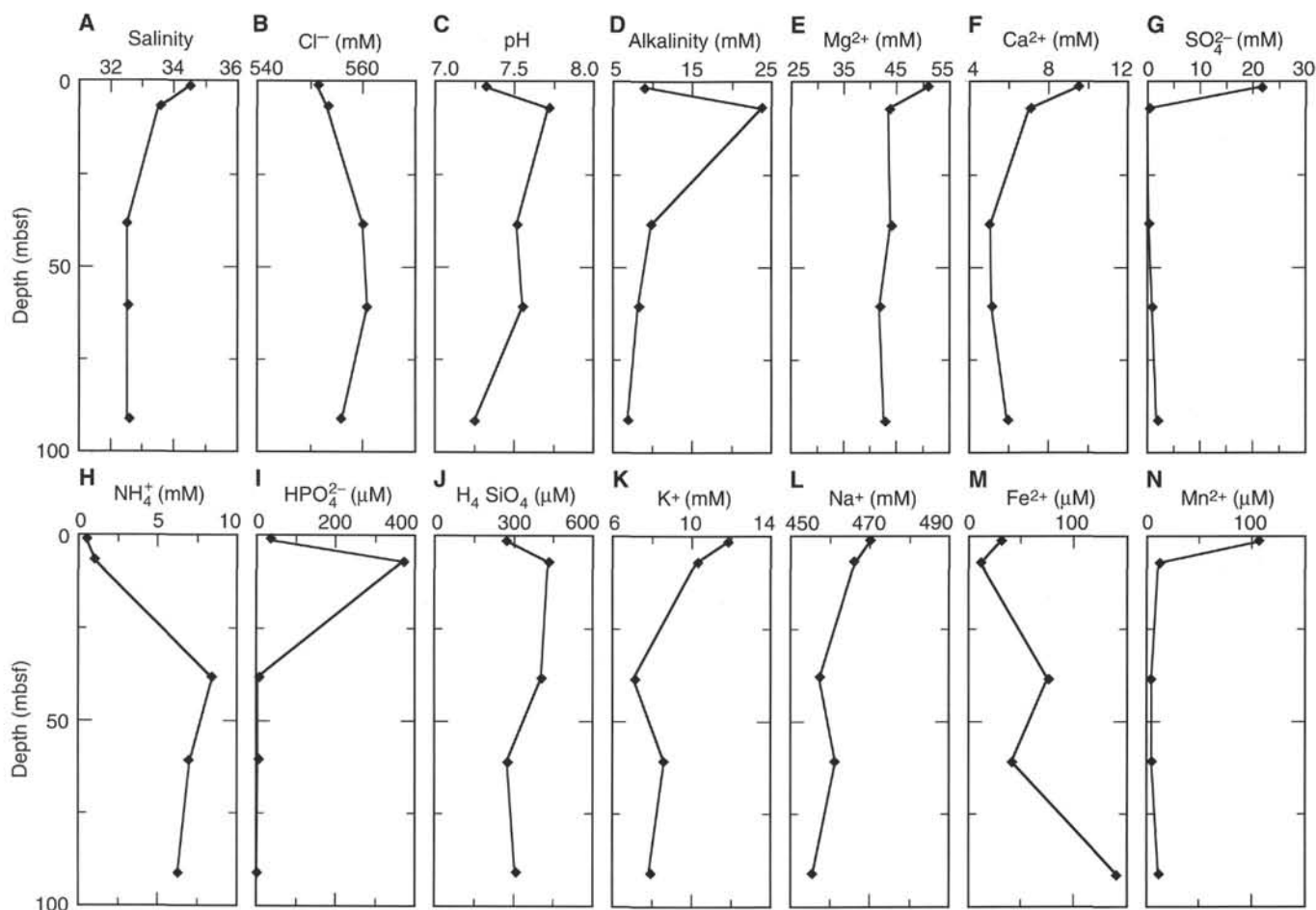


Figure 21. Downhole variation in pore-water chemistry. A. Salinity. B. Chloride. C. pH. D. Alkalinity. E. Magnesium. F. Calcium. G. Sulfate. H. Ammonium. I. Phosphate. J. Silica. K. Potassium. L. Sodium. M. Iron. N. Manganese.

largely variations within individual cores, and steps in the water content profile coincide with core breaks. Over the depth interval sampled, the range and pattern of water content variation in Hole 943A is consistent with that of silty clay at other Amazon Fan sites.

The porosity profile matches that of water content (Fig. 22). Porosity decreases downhole from 80% at 3.87 mbsf to 51.3% at the base of the hole. The general wet-bulk density increase from the top to the base of Hole 943A is 1.41 to 1.93 g/cm³ (Fig. 22). Malfunction of the GRAPE precluded whole-round bulk density measurements. Grain density is more variable at Site 943 than at other Amazon Fan sites, ranging from 2.56 to 2.89 g/cm³ (Fig. 22). The average grain density of the sand intervals sampled is 2.66 g/cm³, and the average for the silty clay is 2.73 g/cm³.

Compressional-wave Velocity

The *P*-wave logger measured compressional-wave velocity for two intervals in Hole 943A, 0.55–5.65 mbsf and 20.80–21.25 mbsf. The deeper interval consists of sand that most likely flowed into the core, and the velocities determined are probably not representative of in-situ velocities. The transverse velocities measured by the PWL averaged 1459 m/s for the upper interval and 1495 for the lower interval.

Shear Strength

Undrained shear strength measurements were made using the motorized shear vane on cores from predominantly silty clay intervals in Hole 943A (Table 10). Compressive strengths were determined with a pocket penetrometer and used to estimate undrained shear strength below 60 mbsf.

Shear strength increases downhole in Hole 943A from 5.7 kPa at 2.13 mbsf to 69.0 kPa at 104.71 kPa (Fig. 23). Between 6 and 34 mbsf, shear strength increases rapidly from 7.2 to 51.8 kPa. The rate of increase slows below 34 mbsf and shows relatively little change downhole to 78 mbsf. Below 78 mbsf, the strength profile is dominated by increases within individual cores (Table 10). The shear strengths estimated from compressive strengths compare well with the lab vane values. The compressive strength estimates range from 44.2 kPa at 61.78 mbsf to 107.9 kPa at 103.47 mbsf.

Resistivity

Longitudinal and transverse resistivity were determined for Hole 943A (Table 11). Longitudinal resistivity increases downhole from approximately 0.25 Ωm near the seafloor to 0.40 Ωm at the base of Hole 943A (Fig. 24). The resistivity increase parallels the downhole porosity decrease, with most of the change occurring between 6 and

Table 9. Index properties at Site 943.

Core, section, interval (cm)	Depth (mbsf)	Water content (%)	Wet-bulk density (g/cm ³)	Grain density (g/cm ³)	Dry-bulk density (g/cm ³)	Porosity (%)	Void ratio
155-943A-							
1H-2, 62-64	2.12	50.0	1.52	2.83	0.76	73.4	2.76
1H-3, 87-89	3.87	58.7	1.41	2.89	0.58	80.1	4.01
2H-1, 90-92	5.20	56.2	1.43	2.57	0.63	76.3	3.22
2H-2, 58-60	6.38	49.7	1.55	2.62	0.78	71.6	2.52
2H-3, 49-51				2.71			
2H-6, 49-51	12.29			2.67			
3H-2, 70-72	16.00			2.66			
3H-4, 74-76	19.04			2.64			
5H-1, 84-86	33.64	30.5	1.86	2.73	1.29	53.9	1.17
5H-2, 84-86	35.14	31.3	1.86	2.72	1.27	54.7	1.21
5H-3, 84-86	36.64	31.5	1.86	2.82	1.27	55.8	1.26
5H-4, 45-47				2.63			
5H-5, 19-21	38.99	30.0	1.87	2.76	1.31	53.6	1.15
7X-1, 90-92	49.70			2.62			
7X-2, 29-31	50.59			2.67			
8X-2, 122-124	60.90	28.7	1.90	2.56	1.36	50.1	1.01
8X-3, 59-61	61.77	25.6	1.97	2.68	1.46	47.3	0.90
9X-1, 86-88	68.66	30.9	1.84	2.65	1.27	53.6	1.15
9X-2, 82-84	70.12	31.2	1.83	2.73	1.26	54.7	1.21
9X-3, 26-28	71.06	29.6	1.87	2.65	1.32	52.1	1.09
10X-1, 67-69	78.07	30.8	1.84	2.69	1.27	53.9	1.17
10X-2, 60-62	79.50	28.7	1.91	2.70	1.36	51.5	1.06
10X-3, 61-63	81.01	29.8	1.87	2.65	1.31	52.4	1.10
10X-4, 79-81	82.69	28.8	1.88	2.67	1.34	51.4	1.06
10X-5, 72-74	84.12	28.7	1.93	2.74	1.38	51.8	1.07
10X-6, 11-13	84.95	29.4	1.88	2.75	1.33	52.8	1.12
11X-1, 100-102	88.00	30.9	1.86	2.80	1.29	55.0	1.22
11X-2, 100-102	89.50	30.6	1.86	2.74	1.29	54.1	1.18
11X-3, 101-103	91.01	30.5	1.86	2.86	1.29	55.0	1.22
11X-4, 102-104	92.52	28.4	1.92	2.75	1.37	51.6	1.07
11X-5, 130-132	94.30	28.5	1.90	2.70	1.36	51.3	1.05
11X-6, 21-23	94.71	28.2	1.90	2.76	1.36	51.4	1.06
12X-1, 106-108	97.66	27.5	1.92	2.77	1.39	50.7	1.03
12X-3, 93-95	100.53	29.0	1.88	2.69	1.34	51.8	1.07
12X-4, 112-114	102.22	28.1	1.90	2.80	1.37	51.7	1.07
12X-5, 86-88	103.46	28.5	1.88	2.68	1.35	51.1	1.04
12X-6, 60-62	104.70	27.8	1.93	2.80	1.39	51.3	1.06

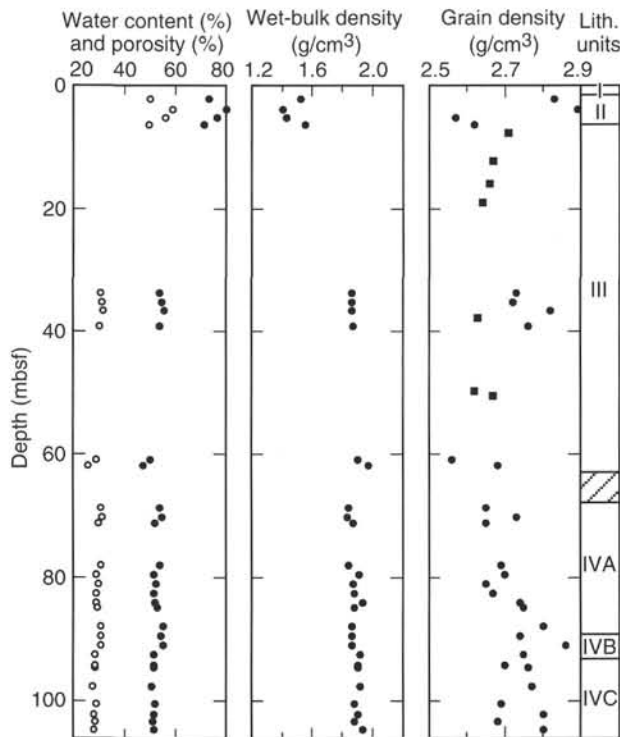


Figure 22. Water content (open circles) and porosity (solid circles), wet-bulk density, and grain density in Hole 943A. Silt and sand sampled only for grain density are represented by squares in the grain density profile.

34 mbsf. Between 34 mbsf and the base of the hole most of the measurements are clustered about 0.40 Ωm.

The variation in resistivity anisotropy is consistent with that determined at other Amazon Fan sites. Negative anisotropy characterizes the color-banded silty clay of Unit II and the silty clay with thin-bedded silt of Unit IV and lower part (below 60 mbsf) of Unit III.

CORE-SEISMIC INTEGRATION

Seismic-facies classification at Site 943 was based on water-gun reflection profiles collected by the *JOIDES Resolution* (2003UTC on 11 May 1994 during Leg 155; Figs. 3 and 25). The reflection record is complex, in part because of side-echoes produced from the channel geometry. Preliminary correlation between the seismic-facies units and the lithologic units is based on the velocity-depth equation determined at Site 931. Seismic-facies Unit 1 is characterized by high-amplitude reflections (HARs) underlying the channel between 0 and 70 ms. This seismic-facies unit is correlative with lithologic Units I, II, and III, which are dominated by sand beds and interbedded mud. The reflections of seismic-facies Unit 1 dip to the east beneath the adjacent levee crest and terminate in diffractions to the west and to the east of the site. The reflections east of the channel could represent either an older channel fill within the levee or side-echoes generated from the sinuous channel morphology (Flood, 1987).

Seismic-facies Unit 2 (70 to 200 ms) is characterized by moderate-amplitude reflections that are discontinuous and subparallel and appear to be nearly horizontal. This seismic-facies unit correlates with lithologic Unit IV, which consists of mud with silt laminae and thin beds characteristic of levee sediment. Two prominent reflections, at 83 and 116 ms, apparently correspond to the contacts between Unit III and Subunit IVA and between Subunit IVA and IVB,

Table 10. Undrained shear strength at Site 943.

Core, section, interval (cm)	Depth (mbsf)	Undrained peak shear strength (kPa)	Undrained residual shear strength (kPa)	Unconfined compressive strength* (kPa)
155-943A-				
1H-2, 63	2.13	5.7	4.3	
1H-3, 88	3.88	4.7	3.5	
2H-1, 90	5.20	8.5	6.2	
2H-2, 58	6.38	7.2	5.6	
5H-1, 85	33.65	51.8	24.9	
5H-2, 85	35.15	61.2	32.0	
5H-3, 85	36.65	45.2	22.6	
5H-5, 20	39.00	58.1	26.6	
8X-2, 123	60.91	59.2	36.6	122.6
8X-3, 60	61.78	58.3	35.4	88.3
9X-1, 87	68.67	46.0	30.9	122.6
9X-2, 83	70.13	47.7	31.6	127.5
9X-3, 27	71.07	62.8	38.4	127.5
10X-1, 68	78.08	47.7	24.1	107.9
10X-2, 61	79.51	52.2	29.0	107.9
10X-3, 62	81.02	60.1	35.2	132.4
10X-4, 80	82.70	64.5	34.3	137.3
10X-5, 73	84.13	90.2	33.5	157.0
10X-6, 12	84.96	75.1	32.4	152.1
11X-1, 101	88.01	68.1	39.6	161.9
11X-2, 101	89.51	69.8	38.7	142.2
11X-3, 101	91.01	76.0	41.5	171.7
11X-4, 103	92.53	78.7	43.8	171.7
11X-5, 131	94.31	73.4	41.5	152.1
11X-6, 22	94.72	83.1	47.0	186.4
12X-1, 107	97.67	64.5	42.5	147.2
12X-2, 86	98.96	46.9	30.4	103.0
12X-3, 94	100.54	61.0	37.7	147.2
12X-4, 113	102.23	69.0	40.7	171.7
12X-5, 87	103.47	76.0	40.4	215.8
12X-6, 61	104.71	69.0	39.3	147.2

Table 11. Electrical resistivity at Site 943.

Core, section, interval (cm)	Depth (mbsf)	Longitudinal resistivity (Ωm)	Transverse resistivity (Ωm)
155-943A-			
1H-2, 63	2.13	0.269	0.245
1H-3, 88	3.88	0.191	0.197
2H-1, 90	5.20	0.246	0.210
2H-2, 58	6.38	0.245	0.239
5H-1, 85	33.65	0.365	0.377
5H-2, 85	35.15	0.369	0.364
5H-3, 85	36.65	0.380	0.382
5H-5, 20	39.00	0.385	0.388
8X-2, 123	60.91	0.451	0.397
8X-3, 60	61.78	0.431	0.409
9X-1, 87	68.67	0.440	0.397
9X-2, 83	70.13	0.385	0.397
9X-3, 27	71.07	0.407	0.388
10X-1, 68	78.08	0.379	0.353
10X-2, 61	79.51	0.420	0.379
10X-3, 62	81.02	0.393	0.387
10X-4, 80	82.70	0.408	0.398
10X-5, 73	84.13	0.412	0.406
10X-6, 12	84.96	0.395	0.382
11X-1, 101	88.01	0.413	0.392
11X-2, 101	89.51	0.403	0.385
11X-3, 102	91.02	0.482	0.398
11X-4, 103	92.53	0.454	0.395
11X-5, 131	94.31	0.377	0.382
11X-6, 22	94.72	0.409	0.394
12X-1, 107	97.67	0.401	0.401
12X-2, 86	98.96	0.429	0.411
12X-3, 94	100.54	0.396	0.415
12X-4, 113	102.23	0.434	0.402
12X-5, 87	103.47	0.390	0.402
12X-6, 61	104.71	0.386	0.410

Note: * = unconfined compressive strength (q_u) can be used to approximate undrained shear strength (S_u) by the relationship $q_u = 2S_u$.

respectively. The reflection at 116 ms is interpreted to correspond to the top of the Purple Channel-levee System located to the west of the site. This reflection has higher amplitude at Site 943 than within the Purple levee flank.

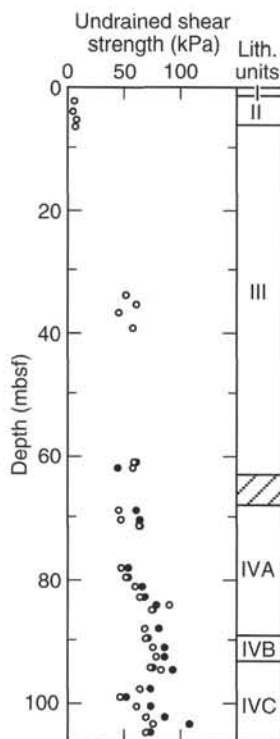


Figure 23. Undrained shear strength (open circles) and assumed undrained shear strength derived from unconfined compressive strength (solid circles) in Hole 943A.

SYNTHESIS AND SIGNIFICANCE

Stratigraphic Synthesis

Holocene Surficial Nannofossil-Foraminifer Clay (Unit I)

Unit I (0–1.58 mbsf) is a Holocene, bioturbated, brown nannofossil-foraminifer clay (Fig. 26). It is similar to that observed at other Leg 155 sites, except that it is interbedded with a 73-cm-thick interval containing a mass-flow deposit underlain by silt-clay turbidites. The mass-flow deposit appears to have slumped off the channel wall. An iron-rich diagenetic crust is developed at 1.28 mbsf. A gray foraminifer-nannofossil clay occurs at the base of the unit.

Latest Pleistocene Bioturbated Mud (Unit II)

Unit II (1.58–6.26 mbsf) comprises bioturbated mud with increasing amounts of black staining below 3 mbsf, associated with a high total sulfur content (0.77%).

Amazon Channel Fill (Unit III)

Unit III (6.26–62.88) consists of mud with interbedded sand. Recovery was only 48%, and some recovered sand appears to be flow-in. At the top of the unit, a fine sand bed containing millimeter-size plant fragments was recovered in two cores, but its original thickness is unknown and it may be mostly flow-in. A large clast of nannofossil-bearing clay occurs at the top of the sand. An interval from 32.8 to 40.2 mbsf recovered mud with abundant beds of silt and sand, commonly with erosive bases. There is a general trend toward thicker beds in the lower part of the interval. The thickest bed recovered is an 81-cm-thick silt bed with mud clasts.

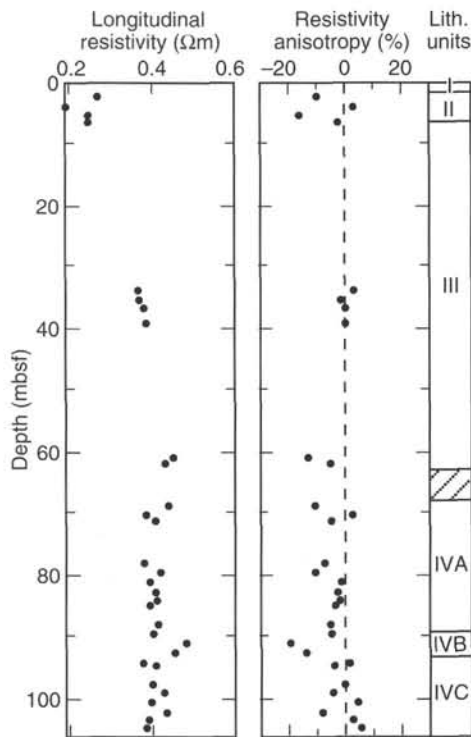


Figure 24. Longitudinal resistivity and resistivity anisotropy in Hole 943A.

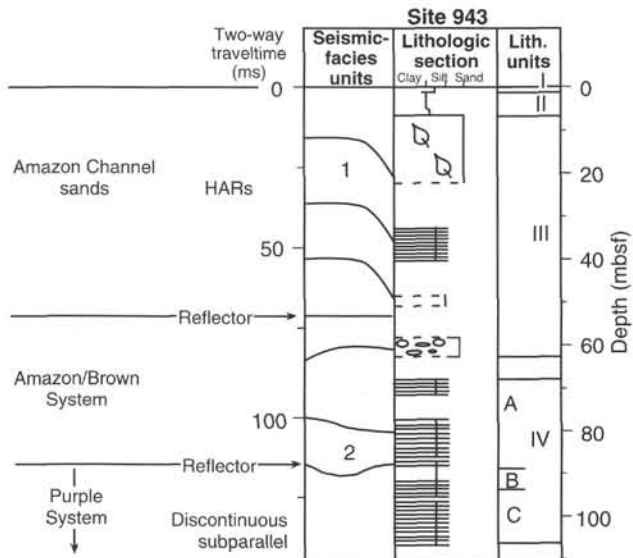


Figure 25. Correlation of lithostratigraphic observations with seismic-facies units and prominent reflections at Site 943.

In the lower part of the unit (58–63 mbsf), a thick bed of silt with minor mud clasts overlies a 19-cm-thick graded bed from very coarse sand to silt, which is underlain by a 2-m-thick bed of clasts of mud with silt laminae in a coarse-sand matrix. This interval below 58 mbsf is correlated seismically with the Amazon-Brown Channel-levee System. The presence of coarse sand and a thick bed with abundant mud clasts, however, is sedimentologically consistent with this interval, marking the beginning of channel deposition. The abundant mud

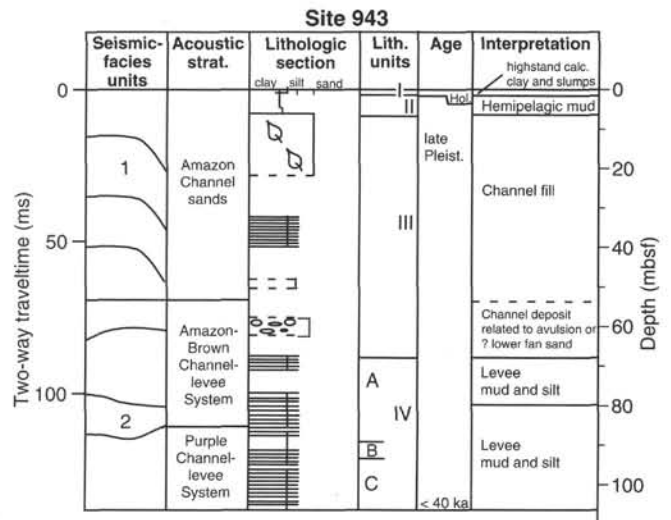


Figure 26. Summary of Site 943 showing (left to right) seismic-facies units, acoustic stratigraphy, schematic lithologic column, lithologic units, age, and interpreted sediment facies.

clasts perhaps result from the breaching and erosion of the levee up-fan.

Levee of the Amazon-Brown Channel-levee System (Subunit IVA)

Subunit IVA (to 89.19 mbsf) consists of mud with abundant laminae and thin beds of silt that is correlated seismically with the Amazon-Brown levee into which the Amazon Channel is cut.

Distal Levee of the Purple Channel-levee System (Subunits IVB and IVC)

Subunit IVB (to 93.29) comprises mottled mud, locally with color banding. Subunit IVC (to base of unit) consists of color-banded mud with frequent beds and laminae of silt. Siderite bands are present in this subunit. Both subunits are typical of the upper part of a levee succession.

Implications

Foraminifer and nannofossil abundances are high in Unit I, except in the resedimented deposits, and low throughout the remaining units. The base of the Holocene was identified near the top of Unit II. *P. obliquiloculata* was not found below the Holocene section, suggesting an age <40 ka for the bottom of the hole. No magnetic excursion was detected at this site. Eight cycles of paleomagnetic inclination and intensity are found between 1 and 3.5 mbsf, and eight more cycles between 34 and 38 mbsf.

This site has provided a channel-fill section through the Amazon Channel on the lower middle fan that can be compared with Site 934, 60 km up-fan. The channel-fill sequence is about 60 m thick, with coarse sand near its base. Otherwise no sediment coarser than fine sand was recovered. The channel overlies levee sediment, suggesting that it has migrated laterally as the levee has accreted. The mottled mud of Subunit IVB at the top of the Purple levee indicates a period of reduced sediment supply.

The presence of a bioturbated mud several meters thick in Unit II indicates that there were no large turbidity current flows in the Amazon Channel for some time before muddy sediment supply was almost entirely cut off by rising sea level in the earliest Holocene. In

Unit I, resedimented deposits are interpreted to be the result of local slumping off the channel wall.

Grain density is more variable at Site 943 than at other Amazon Fan sites, ranging from 2.56 to 2.89 g/cm³. The reason for this is unclear.

REFERENCES*

- Damuth, J.E., 1977. Late Quaternary sedimentation in the western equatorial Atlantic. *Geol. Soc. Am. Bull.*, 88:695–710.
- Flood, R.D., 1987. Side echoes from a sinuous fan channel obscure the structure of submarine fan channel/levee systems, Amazon fan. *Geo-Mar. Lett.*, 7:15–22.
- Flood, R.D., and Damuth, J.E., 1987. Quantitative characteristics of sinuous distributary channels on the Amazon deep-sea fan. *Geol. Soc. Am. Bull.*, 98:728–738.
- Flood, R.D., Manley, P.L., Kowsmann, R.O., Appi, C.J., and Pirmez, C., 1991. Seismic facies and late Quaternary growth of Amazon submarine fan. In Weimer, P., and Link, M.H. (Eds.), *Seismic Facies and Sedimentary Processes of Submarine Fans and Turbidite Systems*: New York (Springer), 415–433.
- Pirmez, C., 1994. Growth of a submarine meandering channel-levee system on the Amazon Fan [Ph.D. thesis]. Columbia Univ., New York.

Ms 155IR-119

*Abbreviations for names of organizations and publications in ODP reference lists follow the style given in *Chemical Abstracts Service Source Index* (published by American Chemical Society).

NOTE: For all sites drilled, core-description forms (“barrel sheets”) and core photographs can be found in Section 4, beginning on page 703. Forms containing smear-slide data can be found in Section 5, beginning on page 1199. GRAPE, index property, magnetic susceptibility, and natural gamma data are presented on CD-ROM (back pocket).